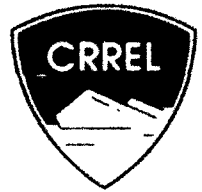


93-3

CRREL REPORT

AD-A266 409

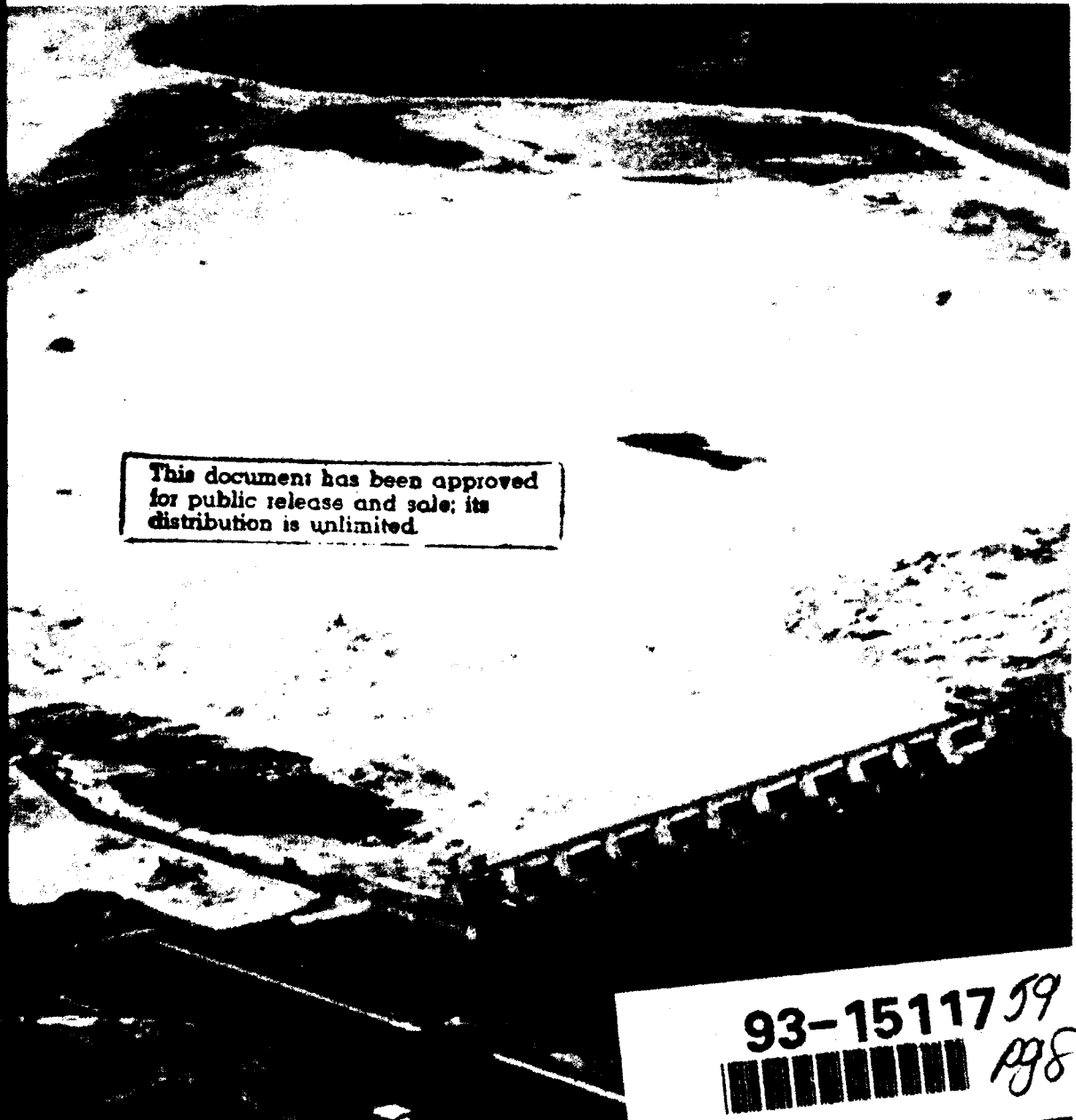


S DTIC
ELECTE
JUL 02 1993
A D

Flow Regulation for Controlled River-Ice Formation

Subash C. Jain, Robert Ettema and Inbo Park

May 1993



This document has been approved
for public release and sale; its
distribution is unlimited.

93-15117 59
1998

93 7 01 05 5

Abstract

Results are presented of a study to determine appropriate methods of flow modification for mitigating ice jam formation in navigable rivers. Based on a review of alternative methods for flow modification, it is concluded that for many rivers, especially large ones, the most appropriate method involves controlled ice-cover formation through the regulation of river flow. Flow discharge and stages would be regulated by controlling the flow releases from reservoirs and flow stages at river dams, such that optimal flow conditions prevail for rapid formation, and subsequent maintenance, of an accumulation ice cover over river reaches in which potentially large amounts of frazil ice may grow. Accumulation covers would be formed of frazil ice pans and floes and, if appropriate, broken ice conveyed from upstream. Existing dams, augmented where needed by navigable ice booms, could serve as retention structures for the development of accumulation covers. A preliminary indication of the feasibility of this method for controlling ice-cover formation on stage-regulated pools of the Ohio River is assessed through the use of a numerical model that simulates ice-cover formation from frazil ice. It is found that this approach holds promise for mitigating jam occurrence, although its implementation necessarily entails management of flow through major portions of the Ohio River. The results of the study are, to a limited extent, generalized to other rivers.

Cover: Severe ice accumulation upstream of Locks and Dam 20, Mississippi River.

For conversion of SI metric units to U.S./British customary units of measurement consult ASTM Standard E380-89a, *Standard Practice for Use of the International System of Units (SI)*, published by the American Society for Testing and Materials, 1916 Race St., Philadelphia, Pa. 19103.

CRREL Report 93-3



**US Army Corps
of Engineers**

Cold Regions Research &
Engineering Laboratory

Flow Regulation for Controlled River-Ice Formation

Subash C. Jain, Robert Ettema and Inbo Park

May 1993

DTIC QUALITY INSPECTED 6

Accession For	
NTIS CRA&I	<input checked="checked" type="checkbox"/>
DTIC TAB	<input type="checkbox"/>
Unannounced	<input type="checkbox"/>
Justification	
By	
Distribution /	
Availability Codes	
Dist	Avail and/or Special
A-1	

PREFACE

This report was prepared by Subash C. Jain and Robert Ettema, Research Engineers at the Iowa Institute of Hydraulic Research (IIHR), The University of Iowa, Iowa City. They were assisted by Inbo Park, Research Assistant at IIHR. The study was funded by the U.S. Army Cold Regions Research and Engineering Laboratory under Grant No. DACA89-86-K-0004.

Technical review of this report was performed by Kevin L. Carey, Dr. George D. Ashton, and Jon E. Zufelt of CRREL.

The contents of this report are not to be used for advertising or promotional purposes. Citation of brand names does not constitute an official endorsement or approval of the use of such commercial products.

CONTENTS

	Page
Preface	ii
Nomenclature	v
Introduction	1
Background	1
Scope of the study	3
Control of river ice formation	4
Control methods	4
Controlled ice-cover formation for the upper Ohio River	8
Numerical simulation of ice-cover formation	10
Flow profile	10
Water temperature variation	12
Frazil ice growth	13
Ice-cover progression	13
Thermal growth of ice cover	14
Numerical results	14
Illustration of simulated ice-cover formation	15
Ice-cover formation in the Hannibal and Montgomery pools	16
Generalized results	19
Conclusions and recommendations	28
Literature cited	29
Appendix A: Expression for coefficients	31
Appendix B: Listing of computer program	33

ILLUSTRATIONS

Figure

1. Formation and drift of frazil-ice pans	2
2. Frazil-generated ice jam impeding navigation in the Illinois Waterway	3
3. Controlled ice-cover formation on the St. Lawrence River	6
4. Controlled ice-cover formation on the Lule River in Sweden	6
5. Ohio River upstream of Hannibal Locks and Dam and its tributaries	7
6. Hydraulic schematic of the Ohio, Allegheny and Monongahela rivers	9
7. Definition sketch	11
8. A weighted, implicit finite-difference scheme	11
9. A computational scheme for method of characteristics	13
10. Ice-cover profiles	15
11. Flow-depth profiles	15
12. Ice-cover development over the Hannibal pool for $Q = 100 \text{ m}^3/\text{s}$	16
13. Ice-cover development over the Hannibal pool for $Q = 600 \text{ m}^3/\text{s}$	17
14. Ice-cover development over the Hannibal pool for $Q = 900 \text{ m}^3/\text{s}$	17
15. Time for ice-cover formation over the Hannibal pool	17
16. Volume of ice in ice cover over the Hannibal pool	18
17. Time for ice-cover formation over the Montgomery pool	18
18. Volume of ice in ice cover over the Montgomery pool	18

Figure	Page
19. Time for ice-cover formation	20
20. Volume of ice in ice cover	26
21. Optimal river discharge for $S_o = 8 \times 10^{-5}$	28
22. Optimal river discharge for $S_o = 2 \times 10^{-4}$	28

TABLES

1. Geometric and flow variables	14
2. Values of empirical coefficients	14
3. Ice and water properties	14

NOMENCLATURE

A	flow area	T	water temperature
B	top width of water surface	T_a	air temperature
C	frazil ice concentration	T_{ao}	constant air temperature
c_p	specific heat of water	T_f	freezing point of water
d	flow depth	T_n	temperature of inflow water at upstream end of pool
e	porosity of individual ice floes	T_o	initial water temperature
e_c	overall porosity of ice accumulation $= e_p + (1 - e_p)e$	T_s	temperature at the surface of the ice cover
e_p	porosity of ice accumulation between ice floes	t	time
E_x	longitudinal diffusivity coefficient	t_A	time for an ice cover to form over a pool
F	Froude number	S_f	friction slope
F_{max}	maximum Froude number for ice-cover progression	s_i	specific gravity of ice
F_c	critical Froude number for juxtaposition	V	flow velocity
g	gravitational acceleration	V	volume of ice
H	$z + d + \bar{\eta}$	x	distance
h_{ia}	energy exchange coefficient at air/ice interface	Y_L	regulated depth of flow at downstream end of pool
h_{wa}	energy exchange coefficient at water/air interface	y	$z + d$
h_{wi}	energy exchange coefficient at water/ice interface	z	bed elevation
k	thermal conductivity of ice	α	$h_{wa}/(\rho c_p d)$
L	latent heat of fusion of ice	β	spatial weighting factor for the Preissmann's scheme
ℓ	channel length	ε	$h_{wa}/(\rho_i L_i d)$
n_c	composite Manning's coefficient	$\bar{\eta}$	equivalent thickness of ice cover $= s_i \eta$
n_b	Manning's coefficient for channel bed	η	ice-cover thickness
n_i	Manning's coefficient for ice cover	$\Delta\eta$	increment of ice-cover thickness
Q	river discharge	η_i	thickness of ice floe
Q_o	optimum discharge associated with minimum time for ice-cover formation	θ	temporal weighting factor for the Preissmann's scheme
Q_n	regulated discharge at upstream end of pool	ρ	density of water
R	hydraulic radius	ρ_i	density of ice
		ϕ_{wa}	net heat flux from water to air, for unit surface area of flow

Flow Regulation For Controlled River-Ice Formation

SUBASH C. JAIN, ROBERT ETTEMA, AND INBO PARK

INTRODUCTION

Although many northern rivers are regulated for the purposes of flood control, navigation, and hydropower generation, few are regulated to mitigate problems arising from ice formation. In some respects this is not surprising, as flow regulation to mitigate ice problems entails an additional tier of constraints on those imposed for ice-free flows. Nevertheless, for rivers that experience frigid winters, the penalties of not regulating to mitigate ice problems can be severe. The upper portion of the Ohio River is one such river. It is prone to severe ice jams that are of potentially major economic consequence.

This study examines the technical (hydraulic) feasibility of regulating river flow to control ice-cover formation so that ice jams do not occur. It was conducted within the context of the U.S. Army Corps of Engineers (COE) River Ice Management (RIM) Program, which is aimed at developing engineering methods for managing navigable rivers that become ice-covered during winter. Although it is primarily focused on ice formation over stage-regulated pools in the upper portion of the Ohio River, the results from this study are generalized to other rivers.

Background

Ice-cover formation on rivers characteristically involves two concurrent processes. One is the genesis of frazil ice from individual crystals formed in supercooled water to ice floes and ultimately to a solid ice cover. The other is static- or border-ice growth in zones of relatively quiescent flow, notably along banks and in backwater areas. Frazil ice typically accounts for the greater part of initial ice-cover volume, but border ice growth plays an important role in modifying flow surface geometry by narrowing it in such a way that, at some critically congested section, frazil floes become lodged and initiate upstream progression of a full, solid ice cover.

Often, ice-cover formation on rivers is remarkably orderly, causing little disruption to the water flow. River water under frigid air becomes supercooled to a few hundredths of a degree centigrade (or Fahrenheit) and is seeded by ice fragments from several sources so that small ice crystals appear. These crystals, called frazil ice, grow as they are conveyed by the water flow. After undergoing several morphological changes, from flocs to slush, which rises to produce ice pans that float at the water surface, frazil ultimately comes to rest as floes of fused pans lodged in an ice cover formed as a more or less single layer of floes accumulated over a river reach. Typically, a cover begins at, and progresses upstream from, a section critically narrowed by border ice growth. Figure 1 illustrates ice-cover formation over the Cedar River in Iowa. The physical properties and growth cycle of frazil ice are described comprehensively in several publications, including those by Ashton (1986), Ettema et al. (1984), Daly (1984a), Martin (1981), and Osterkamp (1978).

Certain flow conditions may preclude the orderly development of an ice cover described above. Instead of coming to rest as an accumulation cover of floes and pans juxtaposed in a single layer, frazil slush and pans transported at relatively high velocities may be swept downstream to form a jam at some location where the channel capacity to convey ice is overwhelmed. The result is a type of freeze-up jam (IAHR 1986). It may develop as a so-called hanging dam beneath an existing ice cover if the frazil is predominantly slush. Alternatively, if the frazil is in the form of pans, slush, some floes, and broken border ice, a jam may develop that thickens and compacts by shoving and collapse. Such a jam is shown in Figure 2. Whichever type of jam occurs, channels become impassable to river traffic and river flow becomes restricted, causing a significant rise in stage that usually results in flooding.

The magnitude and steadiness of water flow have an important bearing on whether an ice cover or an ice jam forms. The influence on ice-cover formation of flow



Figure 1. Formation and drift of frazil-ice pans (a), their retention at a downstream barrier (b), and upstream progression as an accumulation cover (c).

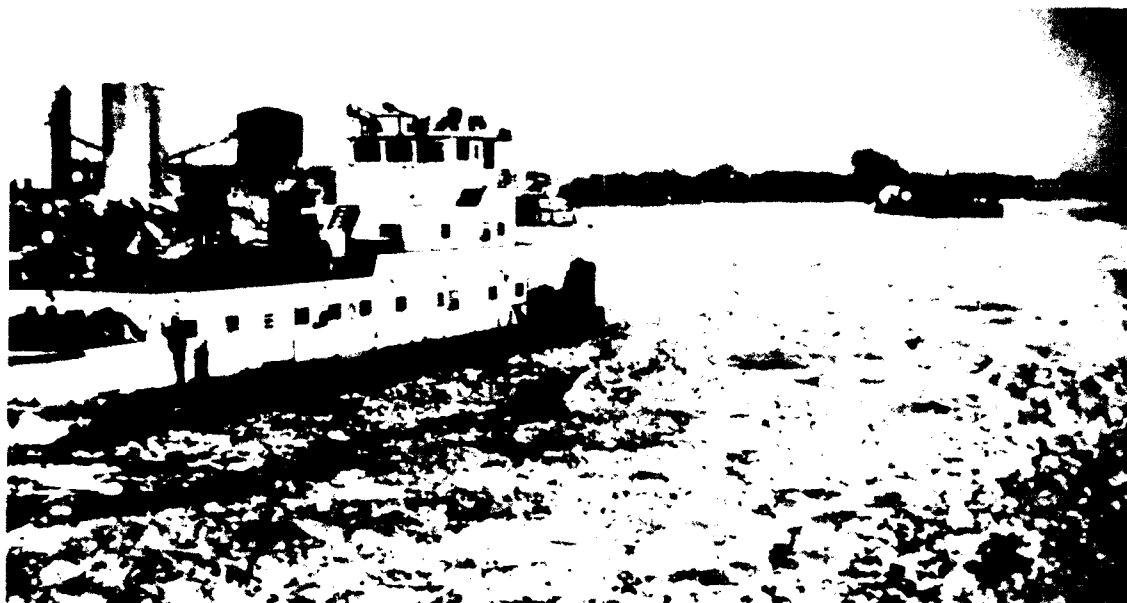


Figure 2. Frazil-generated ice jam impeding navigation in the Illinois Waterway.

magnitude is customarily described in terms of either surface velocity of flow, V_s , or a stability criterion based on flow Froude number, $F = V/(gd)^{0.5}$, in which V and d are the mean velocity and depth of flow, respectively, and g is the gravity acceleration. It is commonly held (e.g., Michel 1978, Ashton 1986) that if V_s is less than about 0.6 m/s for rivers of medium and large depth, flow is insufficiently agitated so that, in calm frigid air, ice crystals growing on the water surface directly form a solid ice cover; for higher values of V , ice-cover formation is as outlined above. Field and laboratory observations (Kivisild 1959, Uzunur and Kennedy 1972) indicate that when F is less than about 0.08 to 0.15 (the larger value corresponding to deep flows; d in excess of about 8 m), individual ice floes and frazil pans gather at a downstream barrier as a more or less single layer that develops upstream, forming a so-called accumulation cover of juxtaposed pans or floes, as described above. Shen et al. (1984) suggest that, for this condition, $F \approx 0.05$. Thickened ice covers and ice jams are attributed to flows with higher values of F . Large discharges may preclude ice-cover formation and contribute to ice-cover breakup. Fluctuations in flow stage may destabilize ice covers or inhibit their formation. An abrupt rise in stage may create uplift forces that lead to ice sheet breaking up.

The calamitous consequences of jam formation were dramatically apparent in January 1978 at Markland Locks and Dam on the Ohio River. The "Markland incident," as it has come to be called, resulted from a sequence of events in which a period of frigid weather, resulting in considerable ice production, was followed by a period of rain that led to a fivefold increase in dis-

charge over 4 days. Ice from frazil growth and the breakup of border ice was conveyed and accumulated as a large jam in the pool immediately upstream of Markland Locks and Dam. Increasing water discharge and stage caused the jam to break and be swept downstream against the dam, where it reformed, causing much damage, destroying portions of the dam and sinking several vessels. The Markland incident and the ice conditions leading to it are described in a detailed report prepared by the Ohio River Division Ice Committee (ORDIC 1978). It raised many issues concerning appropriate operational and structural solutions to managing river ice problems on regulated rivers. In a concerted effort to resolve these issues, the U.S. Army Corps of Engineers initiated the River Ice Management (RIM) Program.

Scope of the study

The general objective of this study was to identify means of hydraulically modifying flow in the Ohio River so as to control frazil ice formation and thereby prevent the occurrence of ice jams. The nature of frazil ice formation and the scale at which it occurs in large, navigable rivers such as the Ohio, however, makes it readily apparent that flow modification necessarily implies regulation of flow discharge and stage in order to create flow conditions that facilitate accumulation-cover formation over extensive lengths of channel in as speedy a manner as is practically possible. In this connection, it is also apparent that structural means of flow modification used without flow regulation would not, under most circumstances, be adequate to control frazil ice formation.

Consequently, this study is specifically aimed at obtaining preliminary indications as to the feasibility of regulating flow for the purpose of facilitating controlled ice-cover formation on stage-regulated pools of the Ohio River and rivers generally. The feasibility of controlled ice-cover formation is assessed through the use of a computational model that simulates one-dimensional flow, frazil ice generation, and accumulation-cover formation on pools of known geometry and slope. It is assumed that accumulation covers form and progress upstream from existing dams or ice booms that act as retention structures. Feasibility assessment is based on the following criteria, which have to be considered at different locations, or regulated reaches, of a river:

- Whether a required discharge can be maintained for the time needed to form an ice cover,
- Whether flow stage restrictions can be adhered to, and
- Whether flow regulation creates any other problems, such as channel scour.

An assessment of feasibility is made for controlled ice-cover formation on two stage-regulated pools of the Ohio River—the pools upstream of the lock and dam installations at Hannibal and Montgomery. As the flow stages for these pools are narrowly constrained to within 1.5 m (4 to 5 ft), this assessment concentrates primarily on discharge regulation.

The numerical model yields information on periods of time for accumulation covers to form, volumes of ice grown, ice-cover profile, and water stage profiles. Information on ice-cover formation times and ice volumes is presented in a generalized format so that it can be applied in assessing the feasibility of controlled ice-cover formation for a range of rivers.

Flow modification to prevent ice jams that result from ice-cover breakup (break-up jams) (IAHR 1986) is not examined here, except insofar as it affects the maintenance of accumulation covers once they are formed. In some respects, flow regulation to prevent ice-cover breakup involves fewer constraints than are required for ice-cover formation. Essentially, it entails attenuation of runoff discharges and the prevention of sudden stage rises so that ice covers do not begin breaking at their upstream end, which leads to a situation where ice discharge increases as the ice-cover breakup progresses downstream. If an ice cover is to break up, it is best that breaking commence at the downstream end so that the ice discharge does not cumulatively increase and remains within the river's capacity to convey it. Where needed, an ice-breaking vessel can be used to instigate ice-cover breaking from downstream. This practice is described by Aleinikov and Korenkov (1972) and Rozsnyoi (1972) for ice-cover breakup on Soviet and Hungarian rivers and by Petkovic et al. (1984) for the Dan-

ube River in Yugoslavia. Deck (1984) cites the use of amphibious craft to break ice on Cazenovia Creek, which flows into Lake Erie.

CONTROL OF RIVER ICE FORMATION

Diverse structures, such as ice booms, weirs, and channel excavations, are often used in attempts to manage the problems associated with river ice formation. They have resulted in modest success, proving more useful for mitigating local ice problems and problems occurring in small rivers and streams. For many rivers, however, ice problems occur simultaneously at several locations or may arise at any location and may be of such a magnitude as to make structural remedies alone inappropriate. Consequently, a question arises as to what approach is appropriate to mitigate these ice problems. If the river in question is regulated, one approach might be to control water discharge and stage such that in conjunction with appropriate structures, flow conditions are suitable for ice-cover formation and maintenance.

The following discussion begins with a brief review of the various structures and techniques that have been implemented to promote ice-cover formation. It then focuses on the feasibility of flow regulation to control ice-cover formation on the Ohio River and on rivers generally.

Control methods

Controlled ice-cover formation usually involves a retention structure to initiate and hold an ice cover and, on occasion, flow modification to ensure that it forms and stays in place. In some instances, use of a retention structure alone has been sufficient to develop an ice cover. For others, flows have had to be modified such that hydraulic conditions were suitable for ice covers to form at retention structures. Flow modification may entail channel alteration and/or regulation of flow discharge and stage.

Ice retention structures serve as surrogate ice edges, or barriers, that both initiate and provide downstream support to accumulation ice covers. They can be either temporarily placed across a channel, such as ice booms, or they may be constructed as fairly massive, permanent fixtures, such as flow-regulation dams. The diverse forms of retention structures that have been used to date are described in detail by Perham (1983). Michel (1971) and Ashton (1986) also provide useful descriptions of retention structures. The St. Lawrence River, more than any other river, has been invested with retention structures for developing ice covers and mitigating jam formation.

Floating ice booms are the best known form of reten-

tion structure. Perham (1983) discusses them at length and illustrates their application at various rivers. Booms have several advantages over other structures:

- They are comparatively inexpensive to build and install,
- They can be removed for ice-free flow conditions, and
- They can be made navigable.

However, they have to be used with due attention to flow conditions and, because of their light construction, to the forces likely to be exerted against them.

At locations where severe jams perennially develop and where the limits of water-level fluctuation are known and suitably narrow, it is sometimes advantageous to construct fixed booms. An advantage of these is that they do not need to be installed each winter, but remain passively in place. One such boom is being used to form and hold ice covers on the St. Lawrence River at Montreal. It consists of fixed piers (somewhat akin to bridge piers) between which float buoyant beams. Pariset et al. (1966) and Lawrie (1972) describe its operation. A similar installation on the St. Anne River, Quebec, is briefly described by Deck (1984). A completely fixed boom is used to assist in ice-cover formation over the Sigalda Reservoir in Iceland (Perham 1983). This structure, however, comprises an 8-m-deep continuous beam that spans the mouth of the Tungnaa River, an outlet of Sigalda Reservoir.

Instead of providing a complete barrier to form an ice cover, it is sometimes feasible to use isolated structures, such as small artificial islands and piers or pilings, to form ice covers. At some locations, notably those where large ice floes or large masses of frazil slush are to be held, it may be possible to precipitate jamming between structures so that the ice acts as its own barrier. When frozen into an ice cover, these structures also serve as point restraints for the ice cover, helping to maintain it throughout the winter.

The mechanics of frazil ice growth and transport have, on occasion, suggested methods for controlling ice-cover formation. Two that are still under investigation entail trapping frazil ice while it is still in the active phase (water is still supercooled) and initiating ice-cover formation close to the zone of initial frazil growth. One technique (Perham 1981, 1983, 1986) involves the use of collector lines draped in a flow to gather frazil ice; when loaded with frazil, the lines become buoyant and float to the flow surface, freeze together, and thereby initiate an ice sheet. Another method (Perham 1983, Foltyn 1986) entails the use of fence booms, or frazil fences, to collect frazil crystals; when the fence clogs with frazil, it retards the flow and becomes in effect a type of weir. Both techniques have met with mixed results. The main drawbacks are that they are limited to

small rivers and streams and, in the case of frazil fences, may cause stream-bed erosion.

Dams and weirs are installed as more or less permanent structures at especially problematical locations. Their essential functions are to reduce flow velocities, so that ice covers can develop over former high-velocity reaches, and, if gated, to act as a downstream barrier that retains ice covers. They are often used in conjunction with floating ice booms and can be designed to different levels of sophistication. The simplest and least expensive form are submerged weirs constructed of loose boulders and stones; their suitability is limited to small rivers and streams. Gated dams or barrages for ice control can be relatively complex and commensurately expensive structures. They are infrequently used, usually as a last resort at sites where jam formation creates particularly severe problems that are of major economic consequence. One example of a gated ice-control dam is Iroquois Dam located near the headwaters of the St. Lawrence River. Its operation is described by Wigle et al. (1981) and is discussed later in this section. Dams or barrages are intended primarily for flow regulation but may also serve as retention structures; indeed, unintentionally, they usually do.

Several concerns may detract from the use of structures as the sole means of modifying river flow. To begin with, flow conditions have to be suitable for ice-cover formation; usually, this means that F should be less than about 0.15. Suitable flow conditions may not be achieved by structural means. Further, ice problems may arise simultaneously at various locations or at any location along some rivers. It may be both physically difficult and uneconomical to place ice control structures at all potential problem locations. The sheer scale of large rivers may preclude the use of control structures: channels may be too wide or too long, large volumes of ice are produced, associated ice loads are large, and so on. In addition, installation of a permanent ice control structure may conflict with use of a river. For example, booms may pose navigation hazards in heavily trafficked rivers, and dams and channel excavations may unacceptably affect fish habitat.

An option afforded by regulated rivers for overcoming some of the foregoing concerns is flow regulation. There are a few cases where this option has been utilized for controlled ice-cover formation. Most have involved non-navigable rivers and ice-cover formation in the vicinity of rapids where large quantities of frazil grow. An important consideration is selecting the appropriate time to regulate flow. For some rivers, there may be few opportunities to control ice-cover formation. In this regard, a key parameter to selecting an appropriate time for ice-cover formation is water temperature in upstream river reaches and reservoirs.

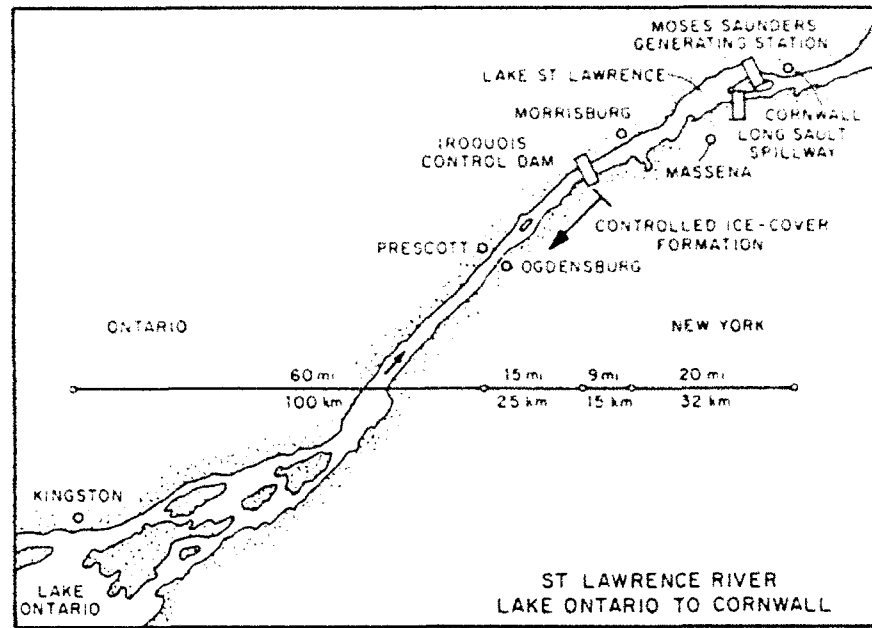


Figure 3. Controlled ice-cover formation on the St. Lawrence River (Wigle et al. 1981).

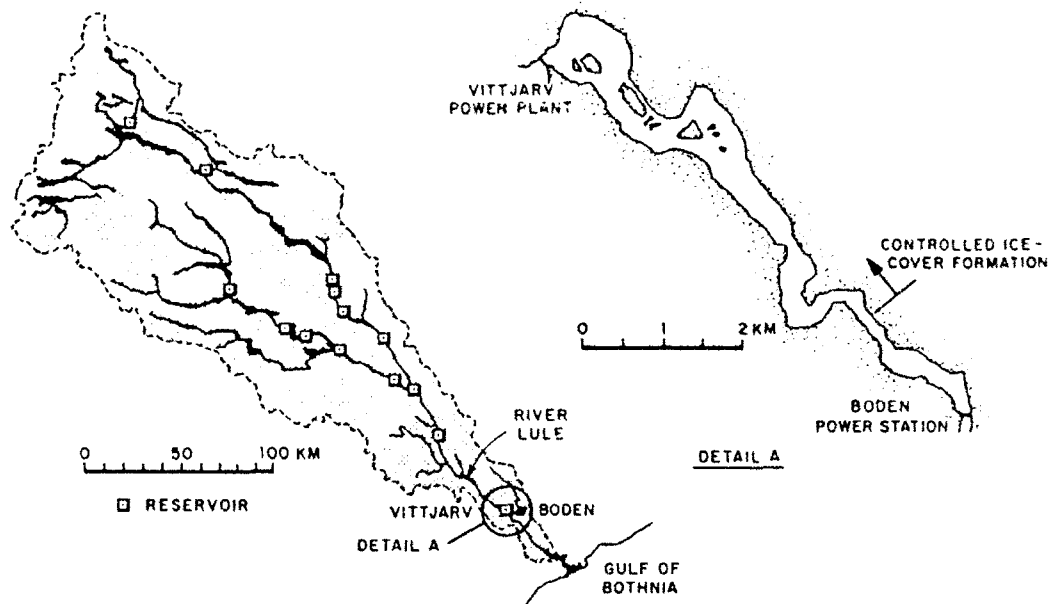


Figure 4. Controlled ice-cover formation on the Lule River in Sweden (Billfalk 1984).

Wigle et al. (1981) describe the measures taken to regulate flow from the outlet of Lake Ontario to eliminate excessive frazil ice growth and to prevent a frazil jam from occurring in the International Rapids section of the St. Lawrence River. Control measures were implemented in order to prevent flooding and to mitigate the deleterious effects of ice on the production of hydro-power from generation facilities located immediately downstream of the section. Figure 3 depicts the channel configuration. An ice cover forms over Lake St. Law-

rence as far as Morrisburg. The control dam is then operated to reduce flow (and flow velocities) and to hold upstream ice, so that the cover can progress to within a few kilometers of the control dam. The dam itself, together with several ice booms located upstream, is used to establish an ice cover for a distance upstream. Shen and Ho (1986) describe the use of a two-dimensional numerical model to simulate frazil-generated ice-cover formation upstream of Iroquois Dam.

Controlled ice-cover formation over a reach of the

Lule River in northern Sweden is described by Jensen (1981) and Billfalk (1984). The river reach of concern is located on the lower portion of the Lule River, upstream of one hydropower plant but downstream of a series of others, as shown in Figure 4. In this case, flow regulation for ice control was complicated by a constraint to maintain power generation. However, the apparently successful approach adopted enables maintenance of power production by prefilling the lower reservoir and using the lower plant to make up the shortfall in power production from the upper plants. A several-day reduction in flow discharge from the upper

portion of the river and use of a boom were effective in forming an ice cover. Earlier attempts at flow modification by means of channel enlargement alone proved to be ineffective in enabling ice-cover formation.

Controlled ice covers have been formed at one location on the Allegheny River, a tributary to the Ohio River (Fig. 5), by means of flow regulation and an ice boom. Deck and Gooch (1984) describe the successful implementation of an ice boom to form and hold a frazil-generated ice cover over several kilometers of the Allegheny River at Oil City. The purpose for forming the ice cover was to suppress excessive frazil ice production

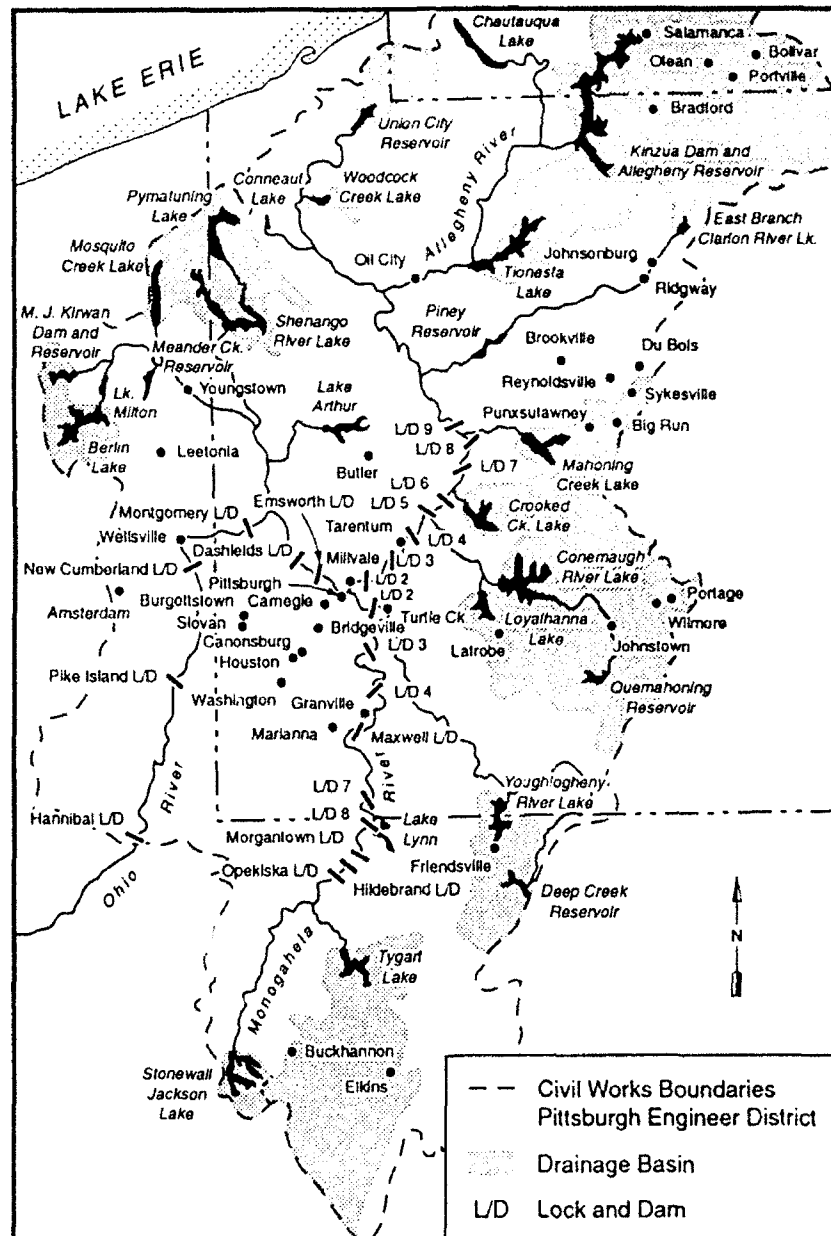


Figure 5. Ohio River upstream of Hannibal Locks and Dam and its tributaries, the Allegheny and Monongahela rivers.

and consequent jam occurrence immediately downstream of Oil City. An important procedure in the cover formation is regulation of flow discharge from Kinzua Reservoir upstream of the boom.

Controlled ice-cover formation for the upper Ohio River

The principal impetus for the present study is the need to prevent the occurrence of large ice jams in stage-regulated pools of the upper Ohio River, here taken to be the Ohio River upstream of Louisville, Kentucky. Figure 5 illustrates a portion of the Ohio River in the general vicinity of Pittsburgh and its tributary rivers, the Allegheny and the Monongahela. In the past, enormous damage has been caused when large jams have formed, led to flooding, subsequently broken loose, and collided with riverside structures. In most instances, the jams have resulted from excessive frazil ice production and from uncontrolled ice-cover breakup.

A survey of ice conditions along the upper Ohio River, which was conducted as part of the present study, leads to the conclusion that the most promising method of preventing ice jams involves the following approach:

Control ice-cover formation through regulation of river flow so that optimal flow conditions prevail for rapid formation and subsequent maintenance of an accumulation ice cover over river reaches in which potentially large amounts of frazil ice may grow. Flow discharge and stages would be regulated by controlling flow releases from reservoirs and flow stages at river dams. Accumulation covers would be formed of frazil ice pans and floes and, if appropriate, broken ice conveyed from upstream. Existing dams, augmented where needed by navigable ice booms, would serve as retention structures for the development of accumulation covers.

This approach necessarily implies coordination of flow regulation for major portions of the upper Ohio River and its tributaries. Before assessing its feasibility for pools comprising the Ohio River, it is in order to present an overview of flow and ice conditions along the upper Ohio.

The Ohio River and its two principal upstream tributaries, the Allegheny and the Monongahela, are major arterial waterways that serve centers of population and industry in the northeastern United States. The three rivers are heavily used for shipping and diverse water-consumption purposes. They are regulated, at least partially, to meet these demands as well as to prevent flooding of adjoining land. Schematically, the rivers can be portrayed as comprising series of navigable pools, punctuated by COE-controlled dams and navigation locks that are linked to an array of flood-control reservoirs in headwater regions or tributary basins. This view is illus-

trated in Figure 6. The pools forming the Ohio and the Monongahela rivers are, with one or two exceptions, stage-regulated by means of gated dams. Upstream of Louisville on the Ohio River there are 14 of these installations. The Monongahela has nine lock and dam installations. The Allegheny River is not stage-regulated, but is broken into a series of eight ungated dams and locks; its upper half is without dams. In each river, the dams are intended to provide navigation channels that are at least about 3 m (9 ft) deep. The pools have negligible storage capacity and are not used for flood control.

Approximately 30% of flow passing through the upper Ohio River is discharge-regulated by means of 25 flood-control reservoirs that are linked to one of the three rivers; 15 reservoirs are operated by the Corps of Engineers. The remaining discharge enters the rivers as unregulated flows from numerous small rivers and streams.

A somewhat unusual hydrologic feature of the three rivers is that their maximum monthly discharges usually occur during winter and early spring, overlapping with the period when they attain minimum water temperatures and form ice. In large part, this feature is attributable to the comparatively dynamic character of winter climate at the watersheds through which the rivers flow. It is not uncommon for cold, northerly air masses to alternate with much warmer, moist air masses from the south and east. The interaction of these air masses is highly unsteady, so that during winter the rivers experience cycles in prevailing air temperature and precipitation. Daly (1984b) presents hydrologic and ice information on the Ohio River.

Because of the variable climatic conditions, ice regimes on the rivers are remarkably dynamic; ice forms during periods of frigid air, and ice covers break up during subsequent periods of warm air accompanied by rain or snowmelt runoff. Ice conditions on the Ohio River have been observed and recorded for over 100 years by the U.S. National Weather Service (ORDIC 1978). Its records show that large quantities of frazil ice may form in the pools as well as border ice along the banks. Although ice forms virtually every winter on the Allegheny and the Monongahela rivers and the uppermost pools of the Ohio, the frequency of ice occurrence diminishes with downstream distance, as the river generally follows a southwesterly course. For example, at Cincinnati, about 500 miles downstream of the confluence of the Allegheny and Monongahela rivers, there is ice on the Ohio an average of 7 out of 10 winters; however, the ice is usually in the form of drifting frazil pans and floes, and the river is only frozen over about 14% of winters.

Detailed survey charts of ice conditions on the Ohio, the Allegheny, and the Monongahela were prepared by

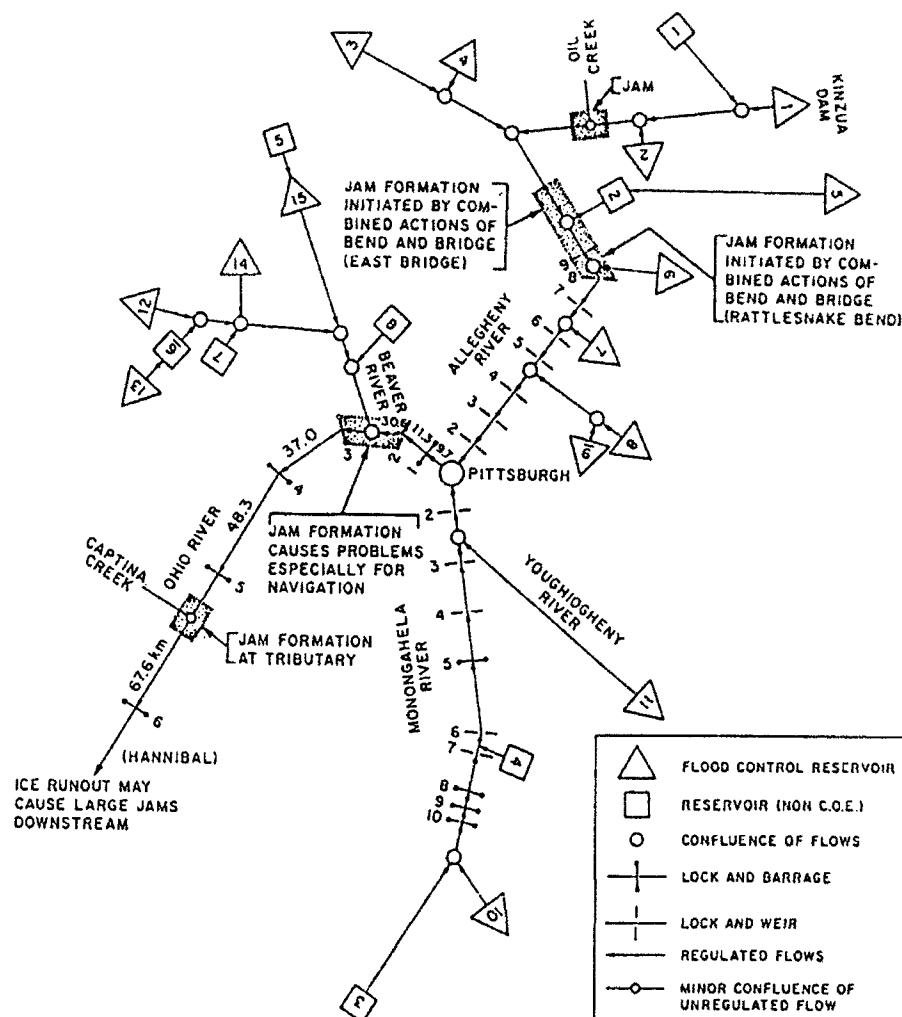


Figure 6. Hydraulic schematic of the Ohio, Allegheny, and Monongahela rivers.

the COE for the winter of 1984–85 (Gatto et al. 1986). The charts reveal that, for the comparatively mild winter of 1984–85, the Allegheny and Monongahela rivers and the Ohio River upstream of Emsworth were covered for periods by fragmented ice covers consisting of frazil ice pans and ice blocks. They also reflect the rather dynamic nature of ice formation on the Ohio. On average, the Ohio River remains navigable by tow-barge vessels about 66% of winters. Navigation on the Allegheny River usually ceases during the months of January and February. The Monongahela, located south of the Allegheny River and flowing northward, typically remains navigable throughout winter.

Significant amounts of ice may enter the upper reaches of the Ohio River and all of the Allegheny and Monongahela rivers from their numerous small tributaries. Being relatively small water bodies, such tributaries cool rapidly and produce ice in most winters. The ice on them also breaks up and is conveyed to the Ohio, often before the ice on that river has broken up.

Prominent among the problems arising from ice formation on the Ohio, Allegheny, and Monongahela rivers are those attendant to ice jams; a summary of ice problems on these rivers is given by Zufelt and Calkins (1985). For the Ohio River, the economic consequences of these problems are exacerbated by its heavy use and, relatedly, by its passage through extensively inhabited and industrialized regions. The Markland incident, recounted in detail by the Ohio River Division Ice Committee (ORDIC 1978), provides stark testimony to the damage that can be caused by a large jam in the Ohio River. The effects of dynamic climate and the lack of synchronized regulation of major segments of these rivers have led to the troublesome occurrence of ice jams. Some jams recur at several locations on the Ohio and the Allegheny. As indicated in Figure 6, these locations often coincide with the confluence of tributary rivers or, as noted by Zufelt and Calkins (1985), with bends, bridge crossings, islands, and channel constrictions.

Each lock and dam installation is a potential jam site; viz. the Markland incident. If there is no coordination between flow and ice releases along a waterway comprising a series of lock and dam installations and reservoirs, there is the potential for a jam to occur at any installation.

NUMERICAL SIMULATION OF ICE-COVER FORMATION

With appropriate regulation of flow, lock and dam installations could be used as retention structures from which accumulation ice covers could be formed. We will now examine this concept further through numerical simulation of accumulation cover formation.

Numerical simulation of accumulation ice-cover formation resulting from frazil ice generation involves computation of the following:

- Flow profile,
- Water temperature,
- Rate of frazil ice growth,
- Rate of ice cover progression upstream, and
- Ice cover thickening by accumulation and static (thermal) ice growth.

In the present study, one-dimensional unsteady-flow equations are used to determine the first three items. Ice-cover thickness profiles are calculated using algebraic relations involving a stability criterion for ice pans, or flocs, arriving at the leading edge of an ice cover.

An outline is presented here of the formulations, boundary and initial conditions, and computational schemes used in developing the numerical simulation. The following general assumptions are made about frazil ice growth and accumulation ice-cover formation:

- (i) Flow, frazil ice growth, and ice-cover progression can be described in terms of depth-averaged, one-dimensional formulations;
- (ii) The two-layer hypothesis* is appropriate for describing ice-covered river flow;
- (iii) River discharge is kept constant during ice-cover formation;
- (iv) Ice covers form at, and develop upstream from, stage-regulation dams where water stage is held constant;
- (v) Frazil ice forms in the reach, or pool, of a river over which an ice cover is to be formed; no frazil or broken ice is transported from the reach above an upstream dam (which in effect could be considered as also becoming ice covered); and,

* The two-layer hypothesis holds that ice-covered flows in formerly open channels can be treated as two free-surface flows: one with the channel bed as its base, the other with the underside of the ice cover as its base.

- (vi) Border ice growth does not significantly narrow flow surface during accumulation ice-cover formation.

Other assumptions are noted within the description of each component of the simulation model.

One issue that is a major stumbling block in computing ice-cover formation from frazil ice is the lack of information concerning lengths of flow, or flow periods, required for frazil in the form of individual crystals to agglomerate as surface-floating frazil pans. Some research effort has been invested in examining the "rise velocity" of frazil crystals and flocs (Park and Gerard 1984, Wuebben 1984), but the results do not fully address this issue. Another issue concerns the proportions of frazil ice grown that are transformed to frazil pans or frazil slush. Here, too, there are few quantitative guidelines to be implemented in a numerical simulation model. To circumvent these issues, while remaining cognizant of their significance, two further assumptions were made concerning accumulation cover formation. First, it is assumed that all frazil ice grown upstream of an advancing cover goes to form that cover. Second, as a means of accounting for mass of frazil ice grown, cover progression was calculated such that a cover advances in incremental steps equivalent to the computational step length, Δx . For each incremental length of advance, the cover thickens until it attains a thickness equivalent to that of a typical pan, which is assumed to be 102 mm (4 in.). Once the incremental advance has reached this thickness, the stability criterion associated with the juxtaposition of frazil ice pans is applied. Another way of viewing the simulation is that frazil pans were assumed to accumulate at the head of an advancing cover in such a way that the head advances a computational step, Δx , before the stability criterion is applied for accumulation cover formation by juxtaposition. If this criterion is not met, the cover thickens, and flow conditions are modified until it is met. Admittedly, the simulation is not precise, but within the context of a preliminary feasibility study it is tenable and yields meaningful information.

Flow profile

Governing equations

Profiles of flow through rivers with floating ice covers (Fig. 7) are described here using one-dimensional equations of gradually varied unsteady flow. These equations are:

Conservation of liquid-water mass,

$$\frac{\partial Q}{\partial x} + \frac{\partial A}{\partial t} = 0, \text{ and} \quad (1)$$

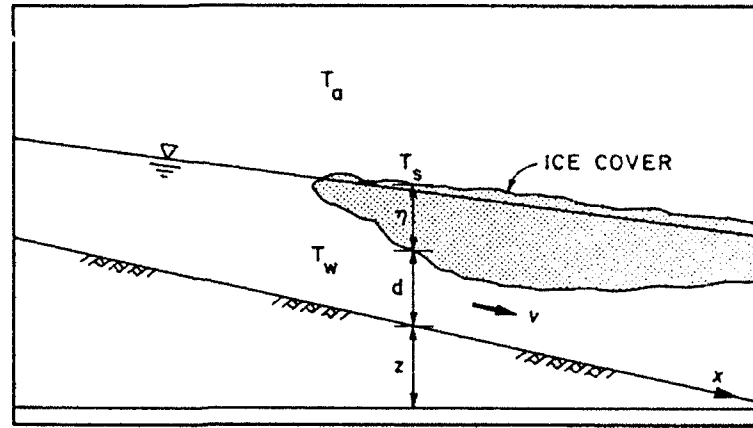


Figure 7. Definition sketch.

Conservation of flow momentum,

$$\frac{\partial Q}{\partial t} + \frac{\partial}{\partial x} \left(\frac{Q^2}{A} \right) + gA \frac{\partial H}{\partial x} + gAS_f = 0 \quad (2)$$

where Q = water discharge
 A = cross-sectional area of flow
 S_f = friction slope
 g = gravitational acceleration
 x = streamwise distance
 t = time
 $H = z + d + \bar{\eta}$
 z = bed elevation
 d = flow depth
 $\bar{\eta} = s_i \eta$ = equivalent thickness of ice cover
 s_i = specific gravity of ice
 η = ice-cover thickness.

Friction slope, S_f , can be expressed in terms of Manning's coefficient as

$$V = \frac{1}{n_c} R^{2/3} S_f^{1/2} \quad (3)$$

where V = mean velocity of flow,
 R = hydraulic radius, and
 n_c = composite Manning's coefficient.

In this report, for ice-covered flow, the composite Manning's coefficient is taken to be

$$n_c = [0.5 (n_i^{3/2} + n_b^{3/2})]^{2/3} \quad (4)$$

in which n_b and n_i are the Manning's coefficients related to flow layers associated with the channel bed and ice cover, respectively (Uzuner 1975). Note that loss of liquid water by freezing to ice is neglected in eq 1, as the volumetric rate of ice growth is much smaller than the water discharge.

Initial and boundary conditions

The upstream boundary condition is constant water discharge Q :

$$Q(0, t) = Q_n \quad (5)$$

The downstream boundary condition is constant water depth at the downstream control section, Y_ℓ :

$$d(\ell, t) + \bar{\eta}(\ell, t) = Y_\ell \quad (6)$$

in which ℓ is the length of river reach. The initial flow profile is obtained by a stabilization process in which the unsteady flow equations for fixed boundary conditions are solved until an assumed flow profile becomes steady.

Numerical scheme

A weighted, implicit finite-difference scheme (Cunge et al. 1980), first developed by Preissmann in 1960, is used to solve simultaneously eq 1 and 2. In accordance with Preissmann's computational scheme (Fig. 8), on

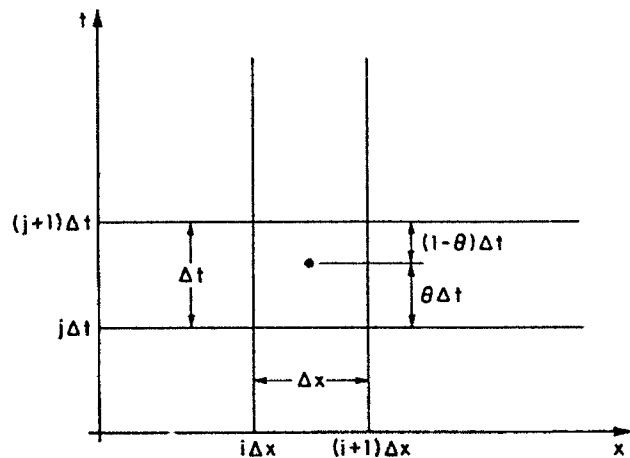


Figure 8. A weighted, implicit finite-difference scheme.

omitting the superscript j for convenience with the understanding that $f(x, t)$ without a superscript corresponds to the value of $f(x, t)$ at the j th time step, any variable $f(x, t)$ and its derivatives are discretized as

$$f(x, t) \equiv \beta f_{i+1} + (1 - \beta) f_i + \theta [\beta \Delta f_{i+1} + (1 - \beta) \Delta f_i] \quad (7)$$

$$\frac{\partial f}{\partial x} \equiv \frac{1}{\Delta x} [f_{i+1} - f_i + \theta (\Delta f_{i+1} - \Delta f_i)] \quad (8)$$

$$\frac{\partial f}{\partial t} \equiv \frac{1}{\Delta t} [\beta \Delta f_{i+1} + (1 - \beta) \Delta f_i] \quad (9)$$

where $\Delta f_i = f_i^{j+1} - f_i^j$
 Δx = length increment
 Δt = time increment
 i = node along x -axis
 j = node along t -axis
 θ = temporal weighting factor
 β = spatial weighting factor.

Cunge and Perdreau (1973) suggested a practical range for θ of 0.6 to 1.0. In the present study, we use $\theta = 0.65$ and $\beta = 0.5$; using slightly different values does not affect the results of the present study.

Equations 1 and 2, on substituting eq 7 through 9, can be written symbolically

$$a_i \Delta y_{i+1} + b_i \Delta Q_{i+1} = c_i \Delta y_i + d_i \Delta Q_i + e_i \quad (10)$$

$$a_f \Delta y_{i+1} + b_f \Delta Q_{i+1} = c_f \Delta y_i + d_f \Delta Q_i + e_f \quad (11)$$

in which $y = z + d$.

The coefficients $a_i, b_i, c_i, d_i, e_i, a_f, b_f, c_f, d_f$, and e_f are given in Appendix A. When eq 8 and 9 are applied to the first $(N-1)$ grid points along the length of the channel (N is the total number of grid points), a system of two $(N-1)$ linear equations involving $2N$ unknowns, ΔQ_i and Δy_i , results. With two boundary conditions (one at the upstream boundary and the other at the downstream boundary for subcritical flows), the number of equations matches the number of unknowns, and hence the system of algebraic equations can be solved to obtain the solution (i.e., y_i^{j+1}, Q_i^{j+1}) at the next time step. The resulting system of equations is solved using the double-sweep method. It is assumed that η is constant within Δt .

Water-temperature variation

Governing equation

Streamwise variation of depth-averaged water temperature can be expressed as a one-dimensional advection-diffusion equation (Brocard and Harlemann 1976) in terms of conservation of thermal energy:

$$\begin{aligned} & \frac{\partial}{\partial t} (\rho c_p A T) + \frac{\partial}{\partial x} (Q \rho c_p T) \\ & = \frac{\partial}{\partial x} \left(A E_x \rho c_p \frac{\partial T}{\partial x} \right) + B \phi_{wa} \end{aligned} \quad (12)$$

where T = depth-averaged temperature of water

B = channel width

ρ = density of water

c_p = specific heat of water

E_x = longitudinal dispersion coefficient

ϕ_{wa} = net heat flux from water to air, per unit surface area of flow.

For Q = constant, and neglecting longitudinal dispersion, eq 12 can be reduced to a simplified form:

$$\frac{\partial T}{\partial t} + V \frac{\partial T}{\partial x} = \frac{\phi_{wa}}{\rho c_p d} \quad (13)$$

Net heat flux ϕ_{wa} is taken to be a linear function of the air and water temperature difference, such that

$$\phi_{wa} = h_{wa} (T_a - T) \quad (14)$$

where h_{wa} is the heat transfer coefficient at the water/air interface and T_a is the air temperature. Herein, $h_{wa} = 20 \text{ W/m}^2\text{°C}$ is used, following the recommendations of Ashton (1986) and Shen and Ho (1986). Substitution for ϕ_{wa} from eq 14 into eq 13 yields

$$\frac{\partial T}{\partial t} + V \frac{\partial T}{\partial x} = \frac{h_{wa}}{\rho c_p d} (T_a - T) \quad (15)$$

Initial and boundary conditions

The following quantities are taken to be constant: initial water temperature along the river reach of interest, temperature of in-flow water with time, and air temperature both above the river reach and with time. In other words,

$$T(x, 0) = T_o \quad (16)$$

$$T(0, t) = T_n \quad (17)$$

$$T_a(x, t) = T_{ao} \quad (18)$$

Numerical scheme

The method of characteristics, with Holly-Preissmann's 4th-order interpolation scheme (Holly and Preissmann 1977), is used to solve eq 15, which can be transformed into a set of two ordinary differential equations:

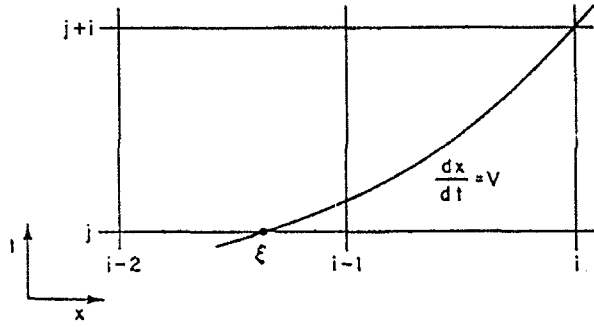


Figure 9. A computational scheme for method of characteristics.

$$\frac{DT}{Dt} + \alpha(T - T_a) = 0 \quad (19)$$

along a characteristic curve (Fig. 9) defined as

$$\frac{dx}{dt} = V \quad (20)$$

In eq 19, $\alpha = h_{wa}/(\rho c_p d)$. Integration of eq 19, from t to t^{j+1} , along a characteristic curve gives (Fig. 9)

$$T_i^{j+1} - T_\xi + \int_t^{t^{j+1}} \alpha(T - T_a) dt = 0 \quad (21)$$

Using trapezoidal integration, eq 21 can be approximated as

$$T_i^{j+1} = T_\xi - \frac{\Delta t}{2} [(\alpha T)_i^{j+1} - (\alpha T_a)_i^{j+1} + (\alpha T)_\xi - (\alpha T_a)_\xi] \quad (22)$$

Unknown values T_i^{j+1} are evaluated using eq 22, and values of T_ξ are interpolated using Holly-Preissmann's 4th-order interpolation scheme, which introduces negligible numerical diffusion and dispersion.

Frazil ice growth

Governing equation

It is assumed that the thermal-energy loss to air of freezing water is balanced by the thermal energy generated by frazil ice growth. The thermal energy generated per unit volume of frazil-laden water is $\rho_i L_i C$, with ρ_i = density of ice, L_i = latent heat of water fusion, and C = volumetric concentration of the frazil. By replacing $\rho c_p T$ with $-\rho_i L_i C$, eq 15 can be used to determine concentration of frazil ice grown:

$$\frac{\partial C}{\partial t} + V \frac{\partial C}{\partial x} = \frac{h_{wa}}{\rho_i L_i d} (T_f - T_a) \quad (23)$$

in which T_f is the freezing temperature of water, herein taken as 0°C.

Initial and boundary conditions

As mentioned above, it is assumed that there is zero influx of frazil ice entering the upstream boundary of the river reach under consideration:

$$C(0, t) = 0 \quad (24)$$

Because initial water temperature in an entire river reach is assumed to be above 0°C, initial concentration of frazil ice is taken as being zero:

$$C(x, 0) = 0 \quad (25)$$

Numerical scheme

Equation 23 is solved for C using the same method of characteristics used to solve for T . Integration of eq 23 along the characteristic curve (eq 20) from C^j to C^{j+1} (Fig. 9) yields

$$C_i^{j+1} = C_\xi - \frac{\Delta t}{2} [(\epsilon T_f)_i^{j+1} - (\epsilon T_a)_i^{j+1} + (\epsilon T_f)_\xi - (\epsilon T_a)_\xi] \quad (26)$$

in which $\epsilon = h_{wa}/\rho_i L_i d$. Values of C_ξ are interpolated using Holly-Preissmann's 4th-order interpolation scheme.

Ice-cover progression

It is assumed that, once initiated, an ice cover progresses upstream in incremental steps of length Δx through accumulation of incoming frazil ice. When Froude number F at the leading edge of the ice cover is less than a critical Froude number F_c for the formation of ice cover by juxtaposition of frazil ice pans, the leading edge progresses upstream as a single layer of pans. Based on field observations reported by Shen et al. (1984), F_c is taken here to be 0.05. The minimum thickness of accumulation cover so formed is the thickness of individual ice pans, n_i , here assumed to be 102 mm (4 in.).

When F exceeds F_c , water flow submerges incoming frazil, which is transported beneath and deposits along the underside of the ice cover. This leads to a gradual increase of ice cover thickness in the vicinity of the ice front. The velocity that is required for ice pans or floes to submerge below the ice cover increases with the increasing thickness of the ice cover. For a given flow depth and velocity upstream of an ice front, a limiting value exists for the accumulation thickness of an ice cover during its progression. Provided F does not exceed a maximum value F_{max} , such that pans do not deposit and thicken an ice cover, an ice cover can progress upstream. The resulting local thickness, η , can be computed from an expression proposed by Michel (1978) as

$$F = \left(1 - \frac{\eta}{d}\right) \left[2(1 - e_c)(1 - s_i) \frac{\eta}{d} \right]^{0.5} \quad (27)$$

where $e_c = e_p + (1 - e_p)e$ = overall porosity of the ice accumulation,
 e_p = porosity of the ice accumulation between ice pans, and
 e = porosity of individual ice floes.

A value of 0.09 is used (following Shen et al. 1984) for the average value of F_{\max} , which corresponds to the maximum value of η/d .

The change in ice thickness, $\Delta\eta_t$, of a reach Δx long in period Δt is

$$\Delta\eta_t = \frac{QC\Delta t}{B\Delta x} \quad (28)$$

If F exceeds a maximum value (F_{\max}), frazil passes beneath the ice cover and is swept downstream until flow velocity becomes low enough for the frazil to rise and come to rest beneath the ice cover, possibly forming a hanging dam of frazil.

Thermal growth of ice cover

Governing equation

As an accumulation cover progresses upstream, it solidifies as porous frazil ice is thermally transformed to monolithic ice and thermally thickens. Thermal thickening is simulated using the following thermal energy equation:

$$\rho_i L_i \frac{d\eta}{dt} = \frac{k}{\eta} (T_f - T_s) - h_{wi} (T - T_f) \quad (29)$$

where T_s = temperature on the top surface of the ice cover,

k = thermal conductivity of ice, and

h_{wi} = heat transfer coefficient at the water/ice interface.

The first and second terms on the righthand side of eq 29 are ice-sheet conduction of thermal energy and thermal energy transfer to the underside of the ice-sheet, respectively.

Numerical scheme

Equation 29 is used to determine ice cover thickening. Assuming a quasi-steady state during a time step Δt , change in ice thickness ($\Delta\eta$) is

$$\Delta\eta_t = \frac{\Delta t}{\rho_i L_i} [h_{ia} (T_s - T_a) - h_{wi} (T - T_f)] \quad (30)$$

where h_{ia} is the heat transfer coefficient at the air/ice interface, here taken to be 20 W/m²/°C (Ashton, 1986,

Shen and Chiang 1984). By equating heat conduction through an ice sheet to heat efflux from its top surface, T_s can be determined as

$$T_s = \frac{kT_f + h_{ia}T_a\eta}{h_{ia}\eta + k} \quad (31)$$

NUMERICAL RESULTS

The simulation model was exercised to determine the times and corresponding volumes of ice required to form frazil-generated accumulation covers over regulated river pools. The parameters varied were pool length, pool bottom slope, and water discharge.

The time required to form an ice cover by frazil ice accumulation over a certain length of a river in a navigation pool depends on a number of variables (Table 1) and coefficients (Table 2) as well as ice and water properties (Table 3). The numerical experiments were carried out with fixed values of the coefficients and the ice and water properties, which are also included in Tables 2 and 3. Though the computer program (Appendix B) was developed for general longitudinal and cross-sectional channel shapes, each stage-regulated pool is

Table 1. Geometric and flow variables.

Variable	Hannibal pool	Montgomery pool
Pool length, l (km)	66	30
Channel width, B (m)	335	305
Downstream flow depth, Y_f (m)	11.5	8.7
Composite Manning's coefficient, n_c	0.033	0.033
Channel-bottom slope, S_o	1.17×10^{-4}	1.97×10^{-4}

Table 2. Values of empirical coefficients.

Empirical coefficient	Symbol	Assigned value
Critical Froude number for cover formation by juxtaposition of ice pans	F_c	0.05
Maximum Froude number for ice-cover progression	F_{\max}	0.09
Heat-transfer coefficient at air/ice interface	h_{ia}	20 W/m ² /°C
Heat-transfer coefficient at water/air interface	h_{wa}	20 W/m ² /°C
Thermal conductivity of ice	k	2.22 W/m/°C
Latent heat of fusion of ice	L_i	333 J/g

Table 3. Ice and water properties.

Physical property	Symbol	Assigned value
Specific heat of water	C_p	4.2 kJ/kg/°C
Porosity of individual ice pans	e	0.4
Porosity of ice accumulation	e_p	0.4
Specific gravity of ice	s_i	0.917
Density of water	ρ	10 ³ kg/m ³
Density of ice	ρ_i	917 kg/m ³

assumed to have constant values of longitudinal slope and Manning's coefficient and to be of constant rectangular cross-section.

Illustration of simulated ice-cover formation

As an illustration of what the numerical model simulates, Figures 10 and 11 show, respectively, predicted profiles of ice cover and flow-depth profile in a representative regulated pool of the Ohio River; the pool length is 24 km. For the sake of clarity, the effect of thermal growth of the ice cover is not included in these two figures. Initial flow profile, indicated by the line ($t = 0$), varies from 8.5 m (28 ft) at the downstream end of the pool to 2.8 m (9 ft) at its upstream end. The unit water discharge is $2.8 \text{ m}^3/\text{s}/\text{m}$ ($30 \text{ ft}^3/\text{s}/\text{ft}$), which yields $F = 0.12$ in the upstream, uniform-flow reach and $F < 0.05$ near the downstream end of the pool, from about $x = 21$ to 24 km. Frazil ice pans start accumulating at the downstream end of the pool where a navigation dam serves to retain them and to regulate flow stage. The

thickness of the ice cover in the reach from $x = 21$ to 24 km is 102 mm (4 in.) during the early period of ice accumulation, because F within this reach is less than 0.05 (the criterion for pan stability and upstream progression of ice cover) and because the ice cover thickness is controlled by simple juxtaposition of frazil pans.

The ice cover did not progress continuously. It advanced until time t_2 , stopped advancing between times t_2 and t_3 , resumed upward progression until time t_4 when it stopped again, and so on, as shown in Figure 10. The inability of the ice cover to progress upstream between times t_2 and t_3 , and t_4 and t_5 , is attributable to F exceeding 0.05 at the leading edge of the ice cover during these periods. However, incoming frazil was deposited under the ice cover, which caused it to thicken and the resultant water depths upstream from it to increase, as shown in Figure 11. When F reduced to 0.05, the ice cover resumed its upstream progression. Throughout the formation of the ice cover, flow stage is maintained constant at the pool's downstream end. However,

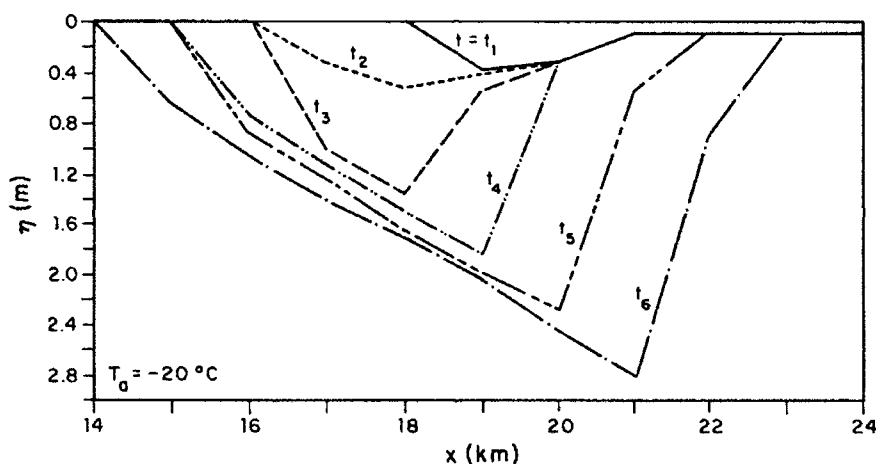


Figure 10. Ice cover profiles.

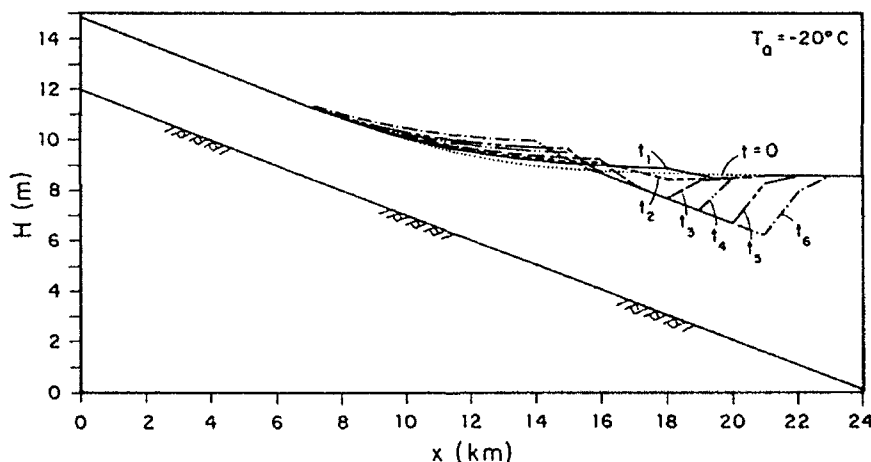


Figure 11. Flow-depth profiles (see Fig. 7 for definitions).

water depth at the leading edge of the ice cover is constant at about 4.6 m, as can be seen in Figure 11, corresponding to $F=0.09$. The incoming ice floes could no longer be deposited in this region and were carried downstream before being deposited beneath the ice cover.

It is evident from this example that the stability criterion for cover progression, $F < 0.05$, significantly affects the overall period of time required for an accumulation cover to progress upstream. Although the sensitivity to this criterion of rate of ice-cover progression is not quantitatively examined in this report, it can be demonstrated that extension of the criterion to $F < 0.15$, as proposed by Ashton (1986), would lead to more rapid ice-cover progression and less ice grown.

In the following sections, attention is concentrated primarily on the overall time required for an accumulation cover to form over pools or reaches of rivers, the total volume of ice grown, and the thickness profile of the resulting accumulation cover.

Ice-cover formation in the Hannibal and Montgomery pools

Numerical experiments were conducted to determine the time required for accumulation covers to form for two pools in the Ohio River, those immediately upstream of the lock and dam installations at Hannibal and Montgomery (Fig. 5). The idealized dimensions and geometries of these pools are included in Table 1. The main difference in their geometries is in their bottom slope, downstream flow depth, and the pool length. The bottom slope, downstream flow depth, and length of the Montgomery pool are respectively steeper, higher, and shorter than those of the Hannibal pool. Ice-cover formation was studied for three air temperatures

(-10 , -15 , and -20°C) and a range of river flows.

Temporal evolutions of accumulation ice covers over the Hannibal pool, under an air temperature of -20°C , are shown in Figures 12, 13, and 14 for three river discharges: 100, 600, and 900 m^3/s , respectively. For the two lower discharges (100 and 600 m^3/s), ice-cover thickness is approximately uniform along the entire pool length, being slightly thicker than 102 mm as given by the condition of pan juxtaposition. The increase in thickness above 102 mm is due to thermal ice growth. In effect, for these two discharges, F at the leading edge of the ice cover never exceeded the assumed critical value of 0.05.

The resulting ice cover is not uniformly thick when river discharge is 900 m^3/s . Instead of forming as a simple juxtaposition of frazil pans, it progressed with a thickened leading edge because there F always exceeded 0.05. The additional thickening of the ice cover due to submergence and deposition of frazil ice delays ice-cover progression.

The time, t_A , required for an ice cover to reach the upstream end of the Hannibal pool is a function of river discharge and air temperature, as shown in Figure 15. The interesting aspect of this figure is that, for a given air temperature, it indicates the existence of an optimum river discharge corresponding to a minimum time required for the cover to form over the pool. Herein such optimal discharges are designated as Q_0 .

The physical explanation for the occurrence of such optimal discharges is as follows. The rate of ice accumulation increases with increasing river discharge, as can be seen by comparing the areas under a curve for $t = \text{constant}$, say equal to 50 hours, in Figures 12 to 14. Thermal growth of the ice cover does not alter the relationship between the rates of ice accumulation and river

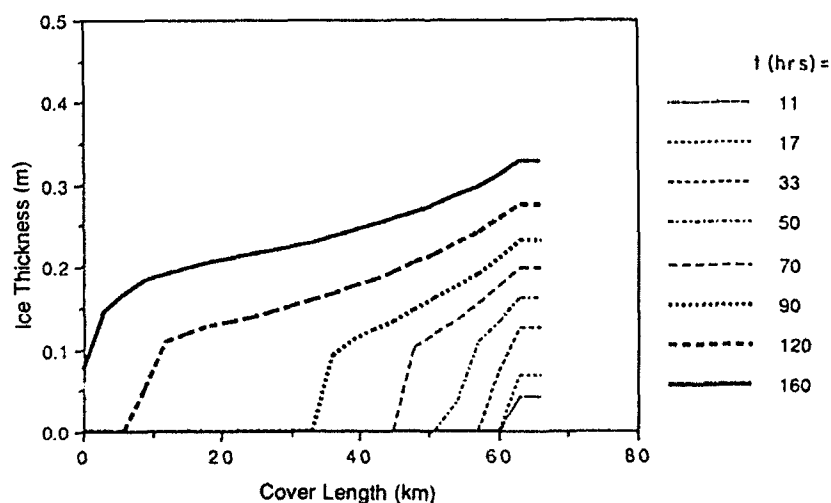


Figure 12. Ice cover development over the Hannibal pool for $Q = 100 \text{ m}^3/\text{s}$.

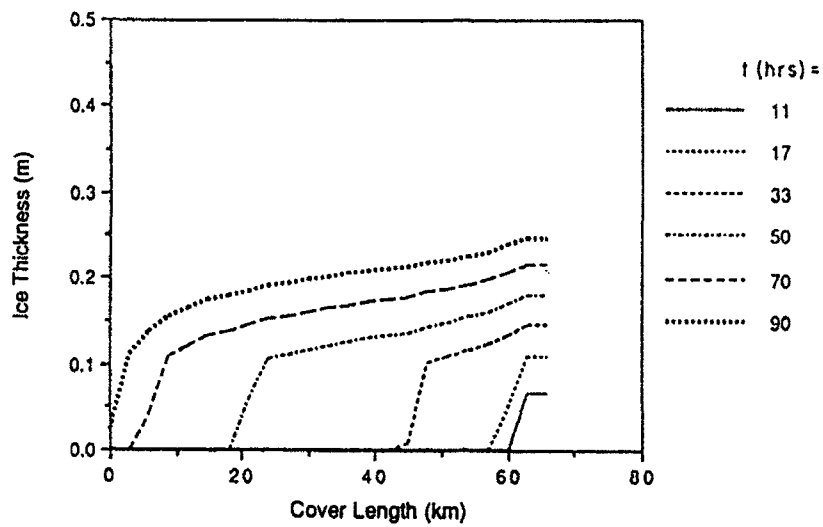


Figure 13. Ice-cover development over the Hannibal pool for $Q = 600 \text{ m}^3/\text{s}$.

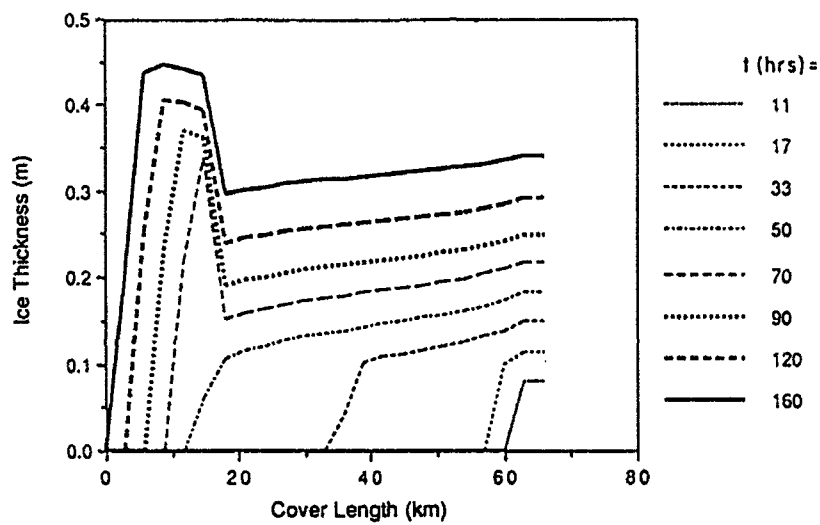


Figure 14. Ice-cover development over the Hannibal pool for $Q = 900 \text{ m}^3/\text{s}$.

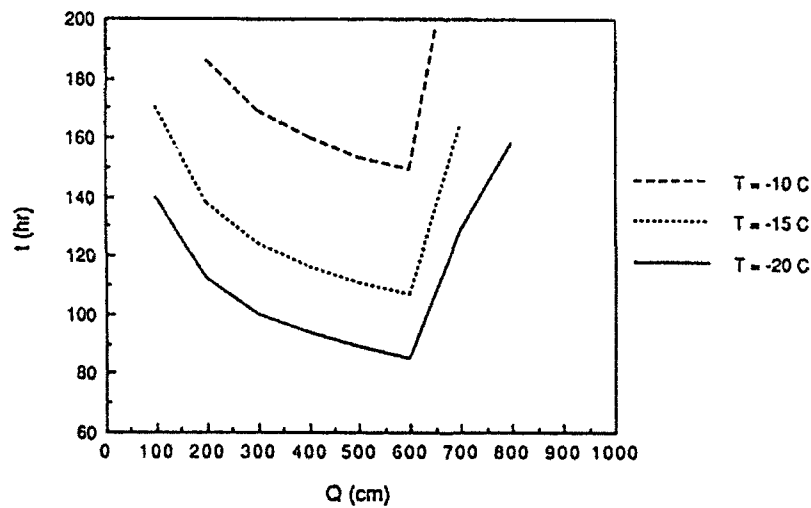


Figure 15. Time for ice-cover formation over the Hannibal pool.

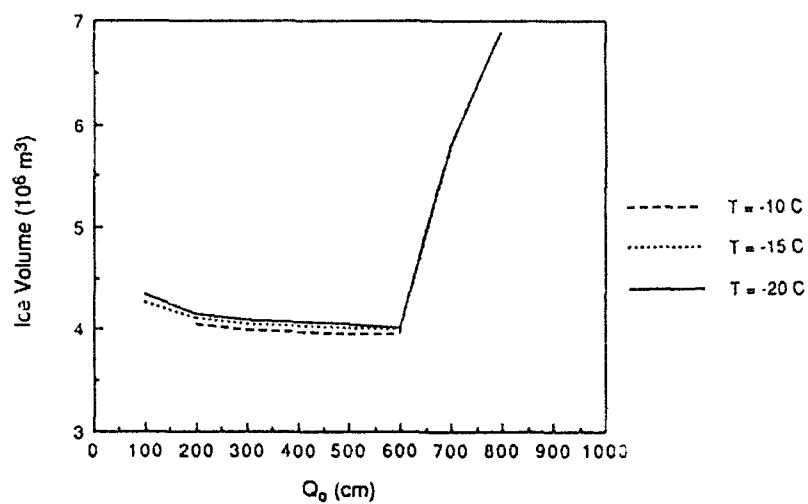


Figure 16. Volume of ice in ice cover over the Hannibal pool.

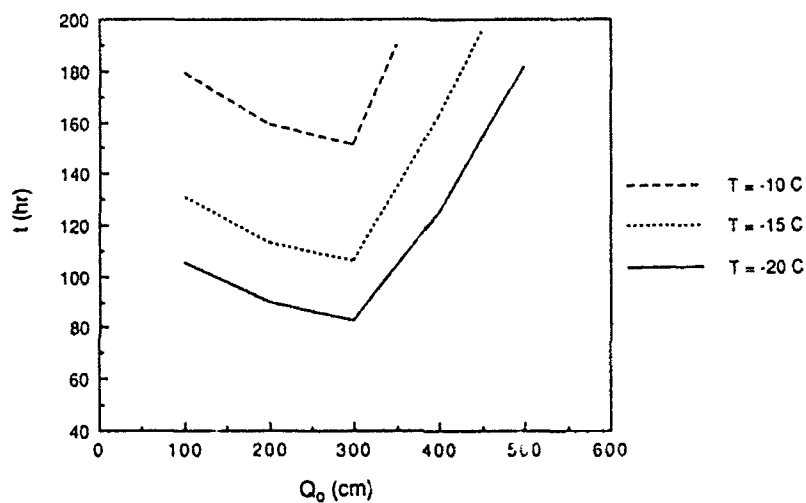


Figure 17. Time for ice-cover formation over the Montgomery pool.

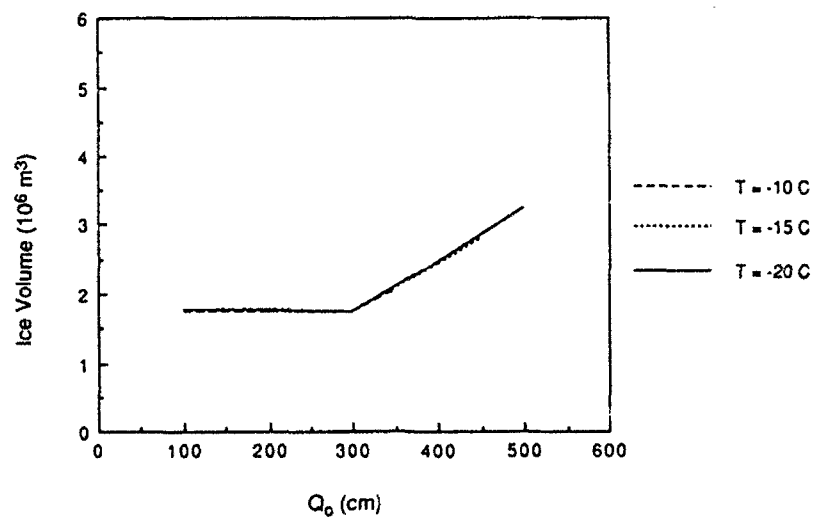


Figure 18. Volume of ice in ice cover over the Montgomery pool.

discharge, though the respective areas do show additional thickening that is attributable to thermal thickening. One would expect the requisite time t_A to decrease with increasing rate of ice accumulation and, consequently, with an increasing river discharge. The inference is correct as long as ice thickness does not change with river discharge, as would be the case when F at the leading edge of the ice cover never exceeds 0.05. This condition would be satisfied for river discharges less than a certain critical value. For river discharges larger than Q_0 , F at river reaches toward the upstream end of the pool would exceed 0.05, causing delay in ice cover progression, as explained earlier, and extending t_A .

Figure 15 also reflects the fact that the rate of frazil ice growth increases with decreasing air temperature and, therefore, t_A decreases with decreasing air temperature for a given river discharge. Interestingly, Q_0 is not sensitive to air temperature because it is controlled by the critical value of $F = V/(gy)^{0.5} = Q/(By^{1.5}g^{0.5}) = 0.05$.

The volumes, V , of ice contained in an ice cover (both as accumulated ice and thermal ice growth) over the Hannibal pool at time t_A for various river discharges and the three air temperatures of -10 , -15 , and -20°C are shown in Figure 16. Volumes of ice grown are almost constant for river discharges less than Q_0 because ice covers form as a single layer of juxtaposed pans with uniform initial thickness. For discharges higher than Q_0 , nonuniform thick accumulation covers form such that V increases with increasing river discharge. The volume of ice at time t_A for a given discharge is not sensitive to air temperature, because ice-cover profiles are primarily controlled by the flow conditions. With decreasing air temperatures, the rate of thermal ice growth increases and time t_A decreases. The net effect of air temperature on ice volume resulting from thermal thickening of the ice cover is insignificant during ice-cover progression.

The numerical experiments produce results for the Montgomery pool similar to those for the Hannibal pool (Fig. 17 and 18). However, because the Montgomery pool is much shorter than the Hannibal pool, lesser times are required to form ice covers, and the resulting volumes of ice are less.

The oldest gauging station nearest to the Montgomery and Hannibal pools is located at Sewickly, Pennsylvania (Fig. 5). The average monthly discharge at this station from December to February ranges from about 250 to 1,250 m^3/s (8,811 to 44,057 ft^3/s). In comparison, the numerical simulation indicates that values of Q_0 for the Hannibal and Montgomery pools are 600 and 300 m^3/s (21,147 and 10,574 ft^3/s), respectively, when flow stage is held at normal operating level at each installation. For higher stages, large values of Q_0 could be used (see *Generalized Results*, below). Because Q_0

for each pool falls within the range of observed mean monthly flows, it appears that flow (primarily discharge) regulation can be used effectively to minimize the duration of ice-cover formation over these pools. The duration of regulation associated with Q_0 for each pool is about 70 to 100 hours (nominally three to four days). An issue arises, however, for a river comprising several pools of varying geometry, Q_0 for one pool, or reach, may not be the same as for others or the river as a whole.

Generalized results

Numerical simulations of ice-cover formation over the Hannibal and Montgomery pools indicate that there exist optimum river discharges, Q_0 , associated with ice-cover formation in minimal periods. The simulations were extended to determine values of Q_0 for a range of regulated river pools under the following conditions:

- (i) Air temperature, $T_a = -20, -15, -10^\circ\text{C}$;
- (ii) Channel slope, $S_0 = 8 \times 10^{-5}$ and 2×10^{-4} (typical for pools upstream of Hannibal);
- (iii) Downstream depth, $Y_L = 8, 12$, and 16 m (nominally 26, 39, and 53 ft, respectively);
- (iv) Pool length, $\ell = 26$ to 162 km (16 to 101 mi.);
- (v) Composite Manning's coefficient $n_c = 0.033$ (based on representative values for the Ohio River and similar large rivers).

The numerical results were obtained for certain combinations of S_0 and Y_L , which yielded upstream flow depths greater than about 3 m.

The curves presented as Q_n vs t_A and Q_n vs V in Figures 19 and 20, respectively, are similar to those presented in Figures 15–18 for the Hannibal and Montgomery pools. The Q_n vs V curves are presented for $T_a = -10^\circ\text{C}$ but, as explained above under *Ice Formation in Hannibal and Montgomery Pools*, are approximately valid for $T_a = -15$ and -10°C , because air temperature has a relatively insignificant influence on V . Variations of Q_0 with Y_L for different pool lengths are shown in Figures 21 and 22, with $S_0 = 8 \times 10^{-5}$ and 2×10^{-4} , respectively. Values of Q_0 for the various flow conditions were obtained from Figure 19. Because the stability criterion for ice-cover progression ($F < 0.05$) does not depend on air temperature, neither do values of Q_0 . Consequently, Figures 21 and 22 are valid for all air temperatures.

Air temperature may in fact affect Q_0 , but in ways not accounted for in the present simulation. For example, by influencing the rate and quantity of frazil ice growth, it might affect the genesis of frazil from crystals to pans, so that all frazil formed does not result in frazil pans, or pan dimensions may differ from the 102-mm (4-in.) thickness assumed herein. In addition, as air temperature influences the solidification, or subsequent freezing, of an accumulation cover as it forms, it could affect

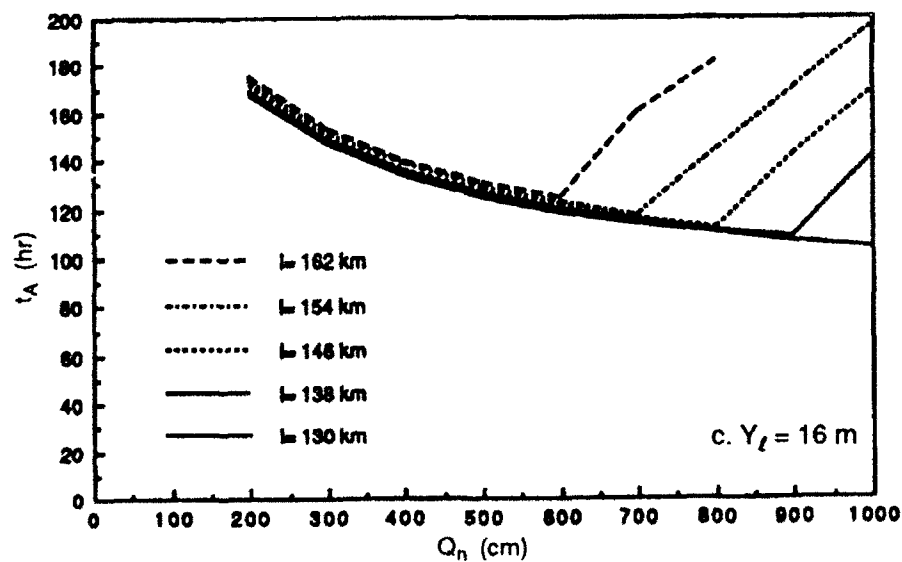
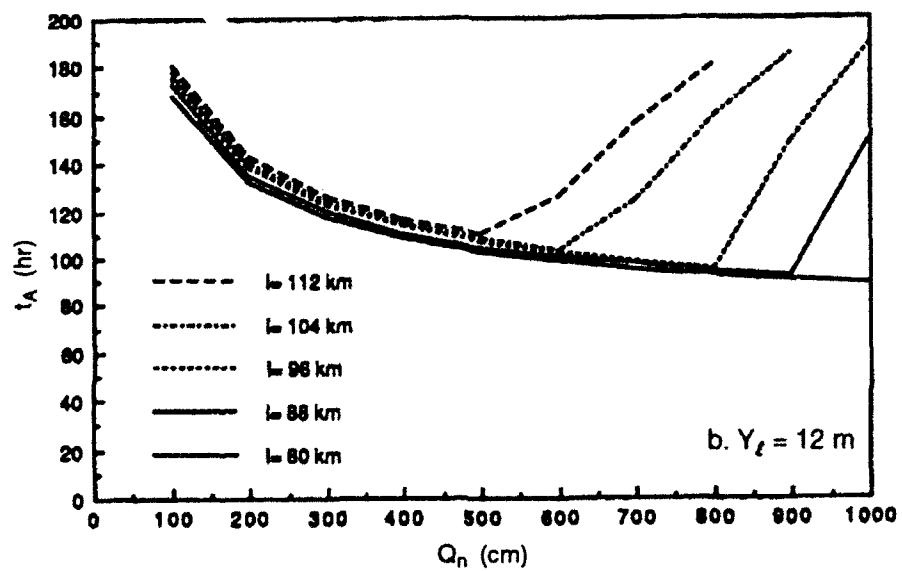
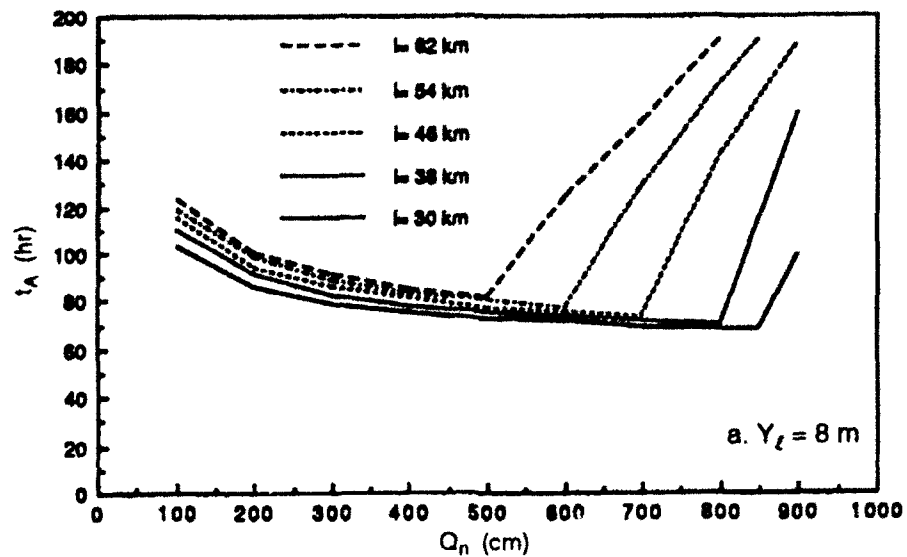


Figure 19. Time for ice-cover formation for $S_0 = 8 \times 10^{-5}$, $T_a = -20^\circ\text{C}$.

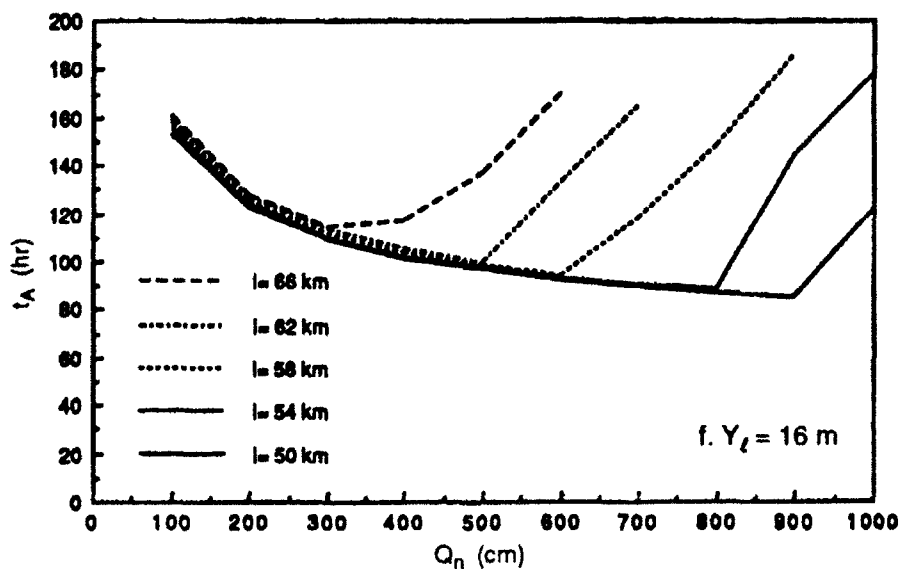
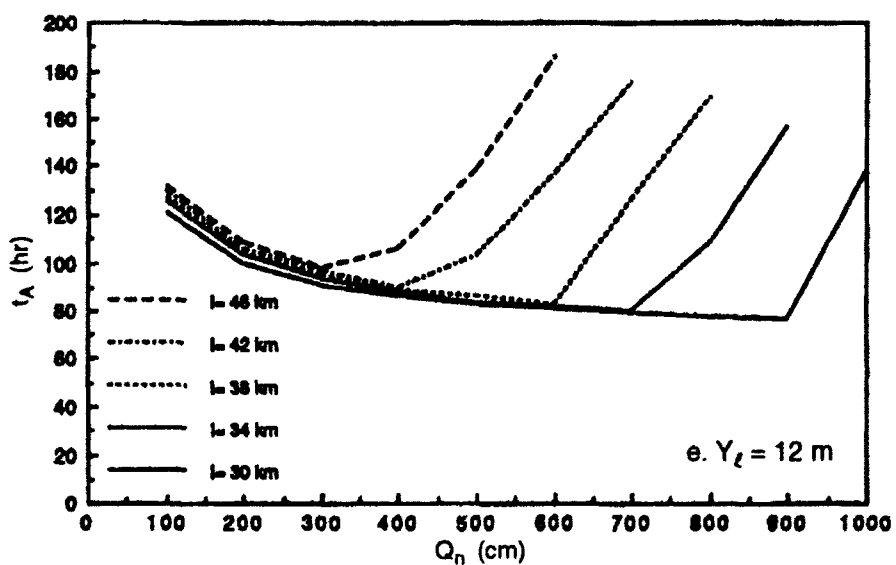
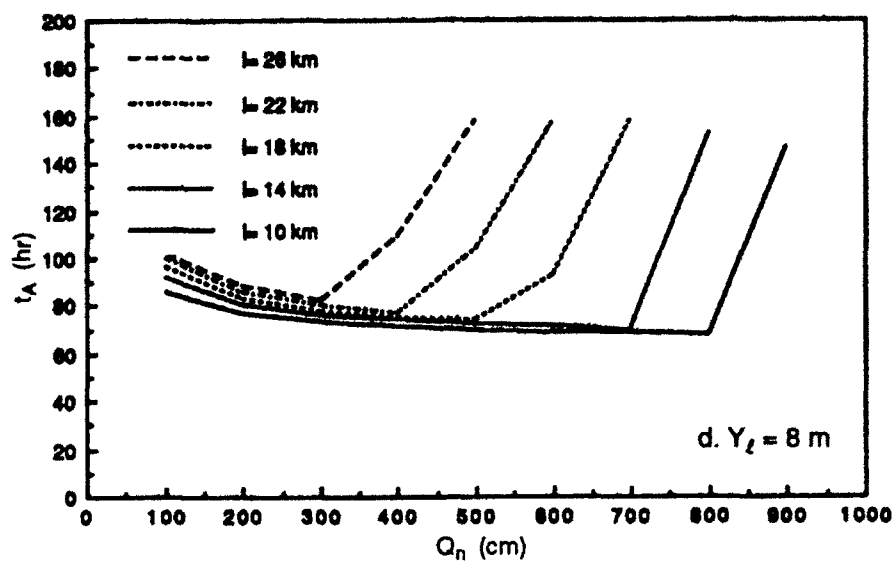


Figure 19 (cont'd). Time for ice-cover formation for $S_0 = 2 \times 10^{-4}$, $T_a = -20^\circ\text{C}$.

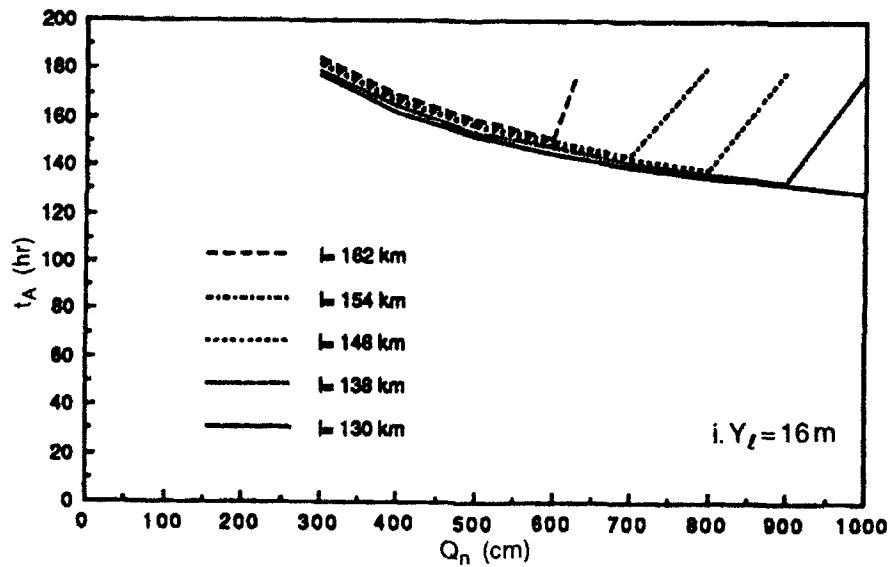
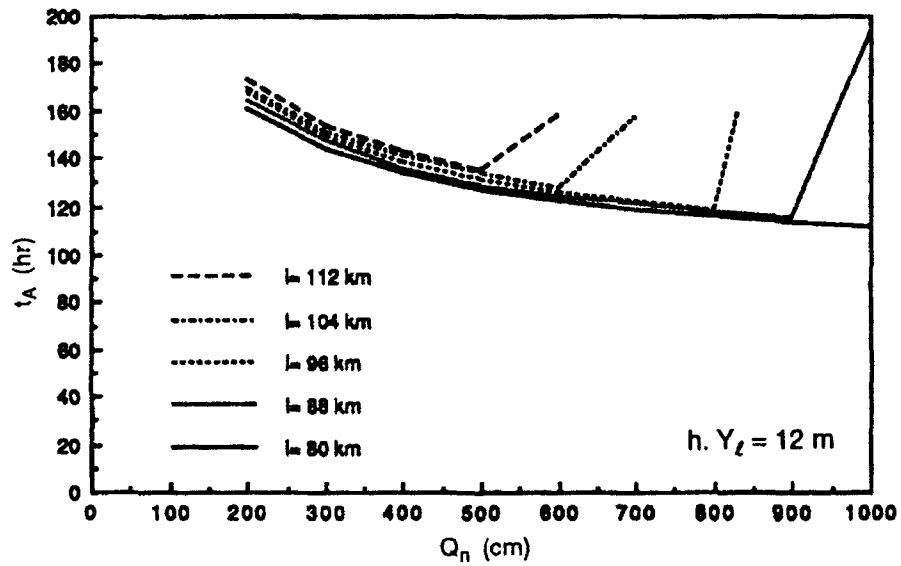
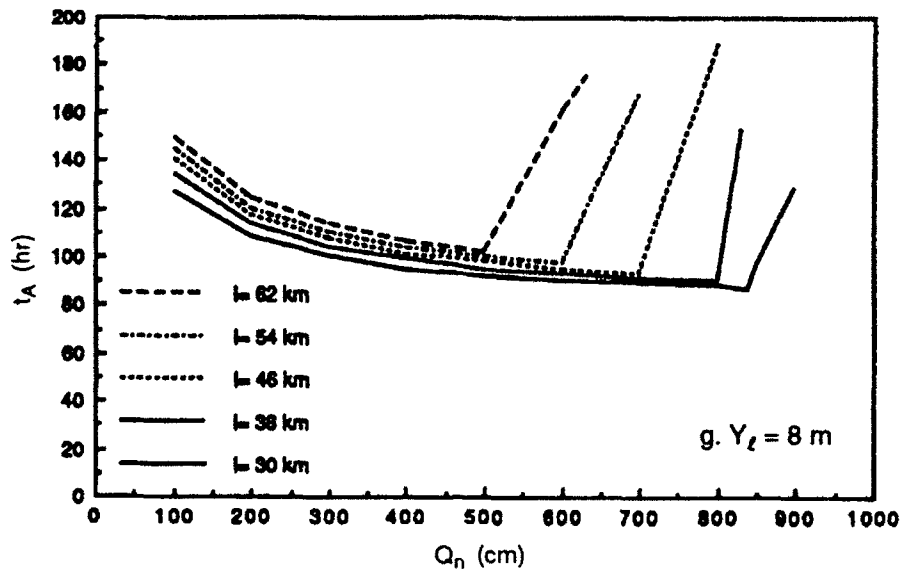


Figure 19 (cont'd). Time for ice-cover formation for $S_0 = 8 \times 10^{-5}$, $T_a = -20^\circ\text{C}$.

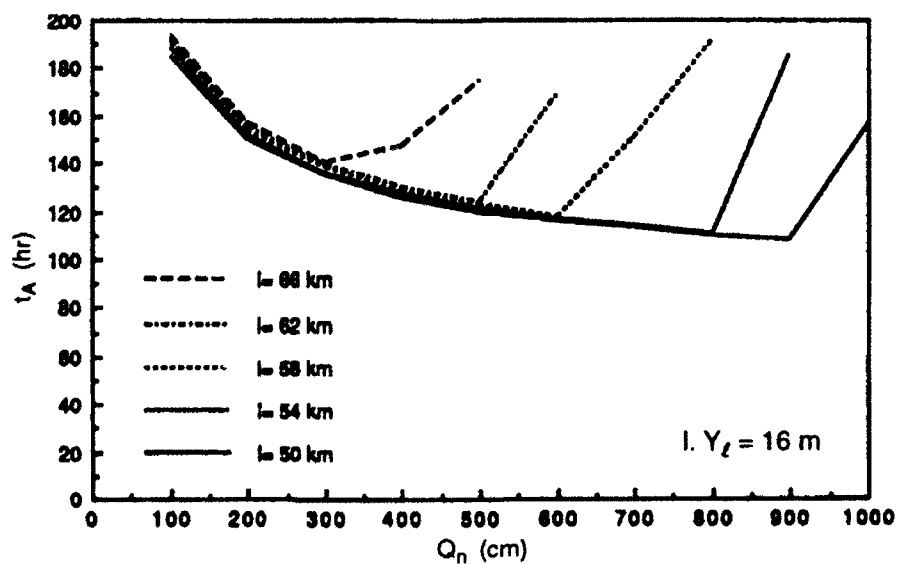
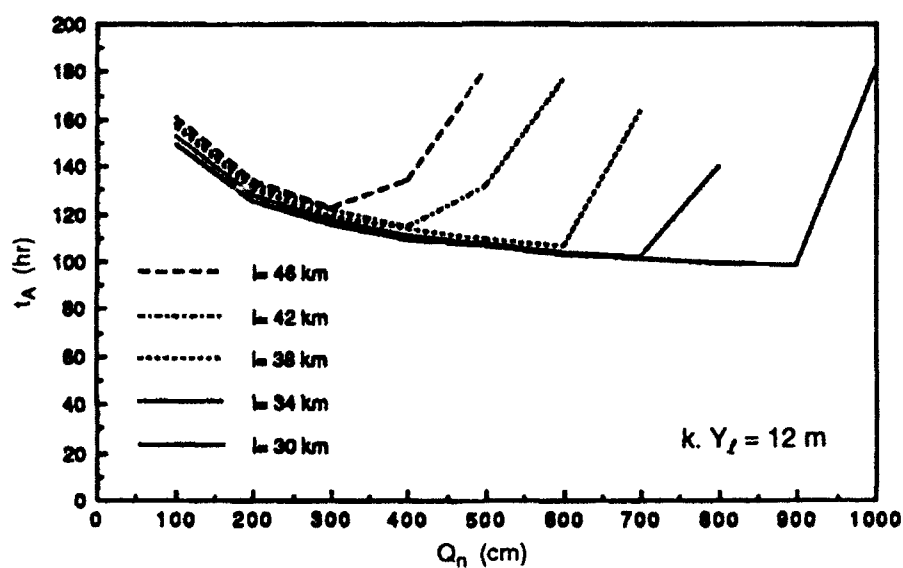
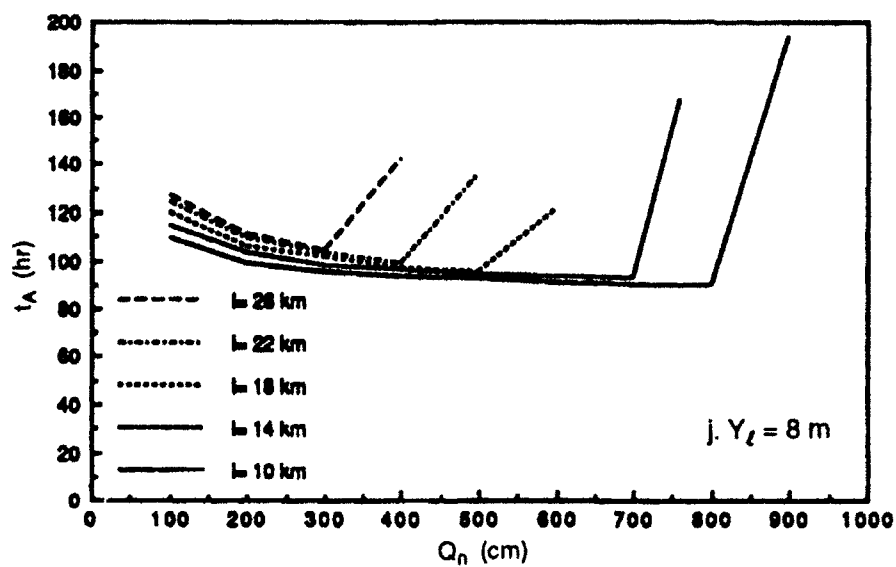


Figure 19 (cont'd). Time for ice-cover formation for $S_0 = 2 \times 10^{-4}$, $T_a = -15^\circ\text{C}$.

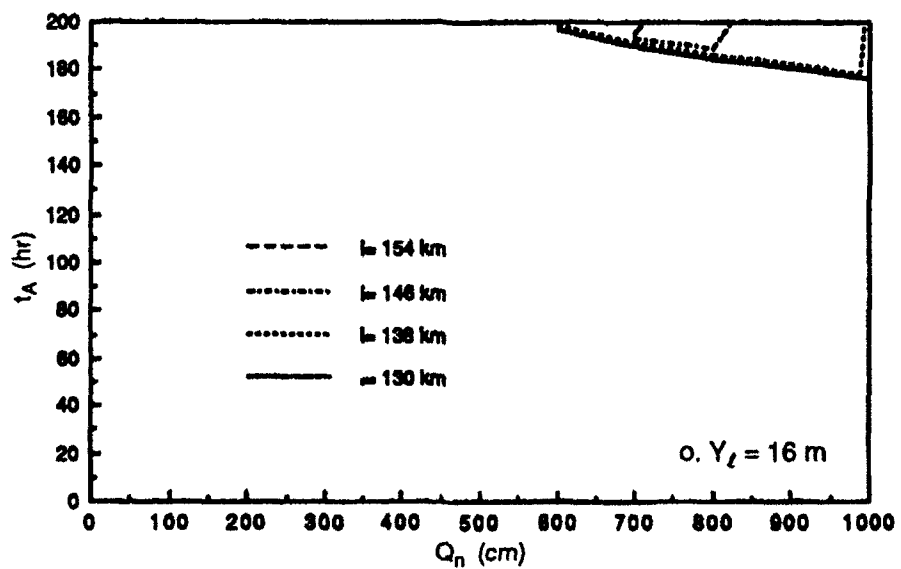
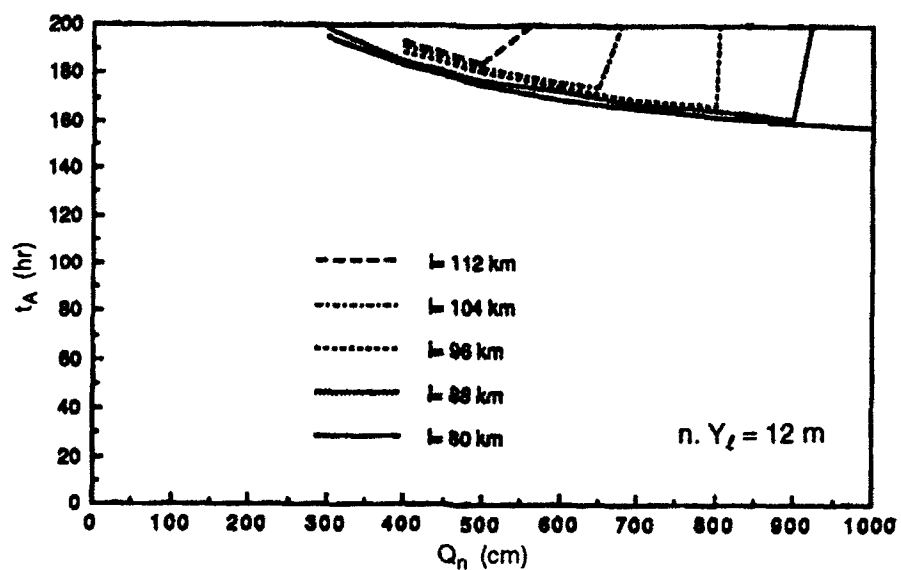
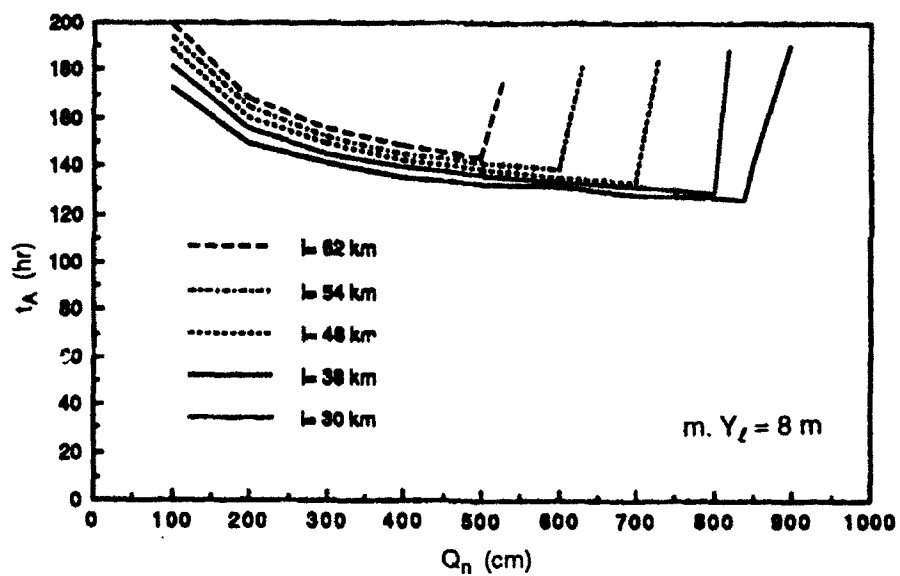


Figure 19 (cont'd). Time for ice-cover formation for $S_0 = 8 \times 10^{-5}$, $T_a = -10^\circ\text{C}$.

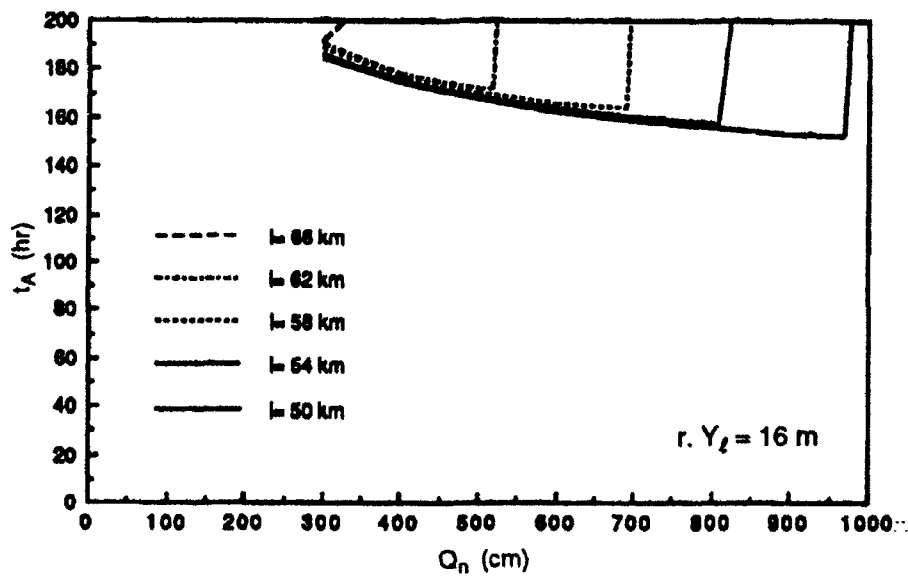
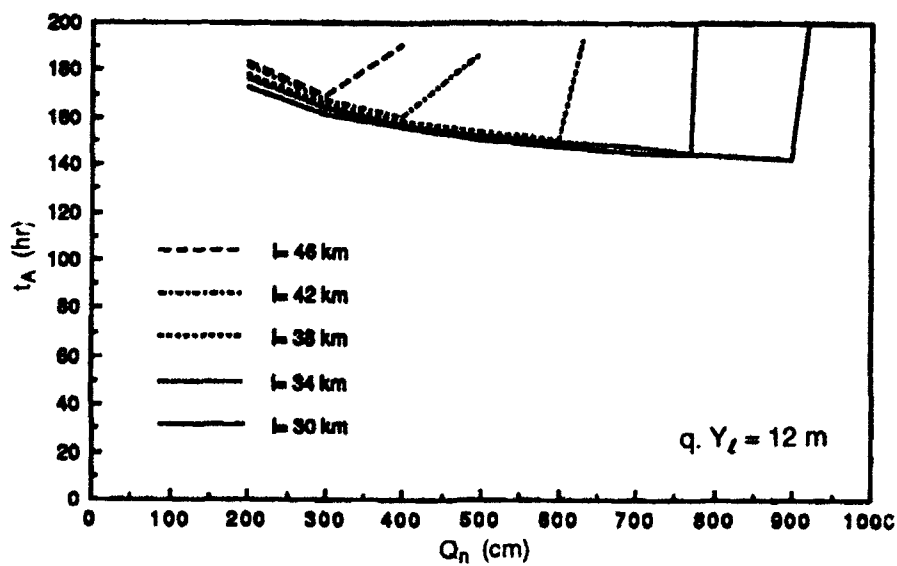
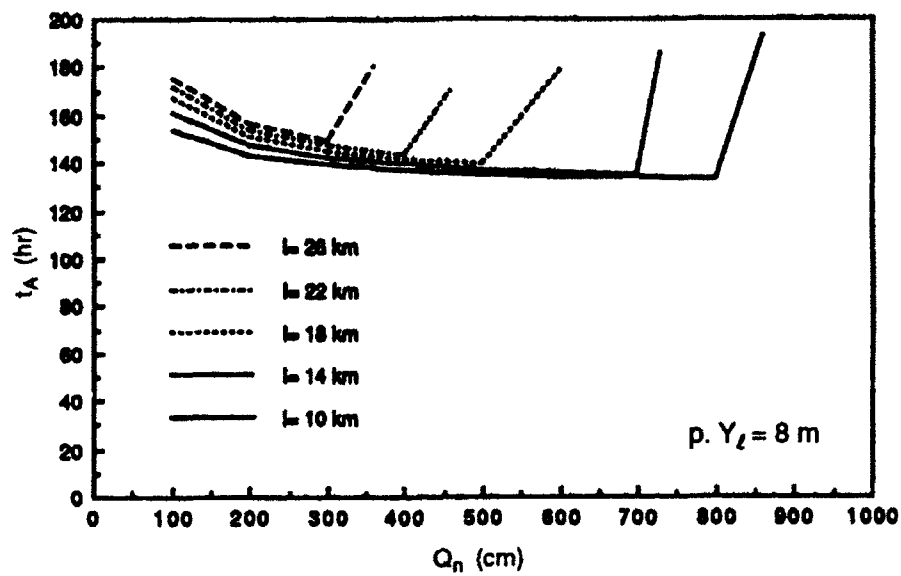


Figure 19 (cont'd). Time for ice-cover formation for $S_0 = 2 \times 10^{-4}$, $T_a = -10^\circ\text{C}$.

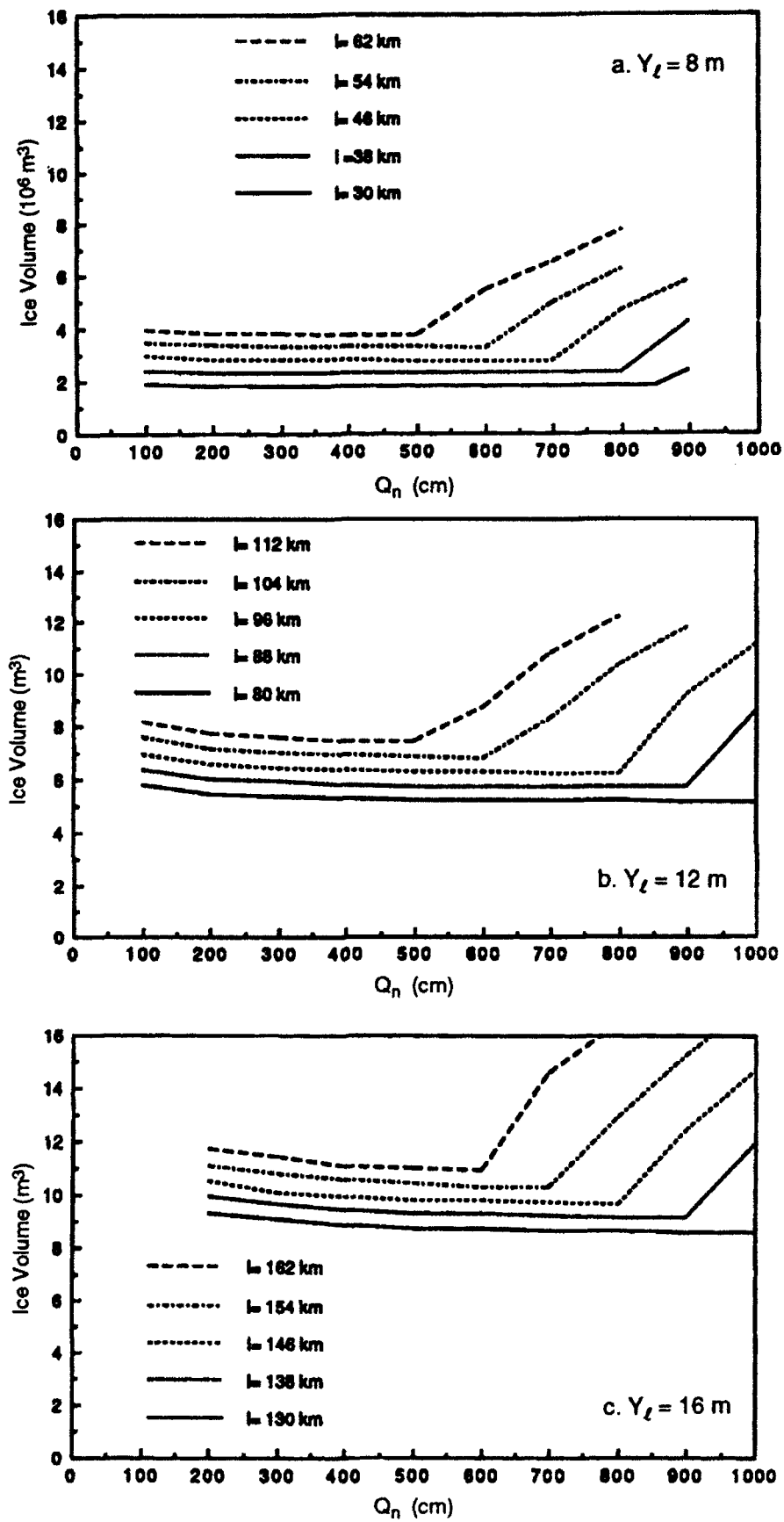


Figure 20. Volume of ice in ice cover for $S_0 = 8 \times 10^{-5}$, $T_a = -20^\circ\text{C}$.

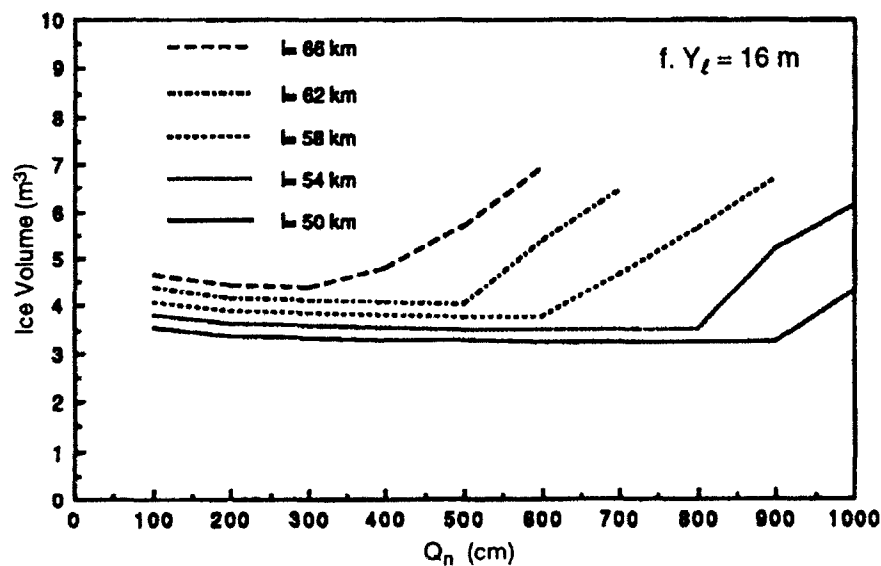
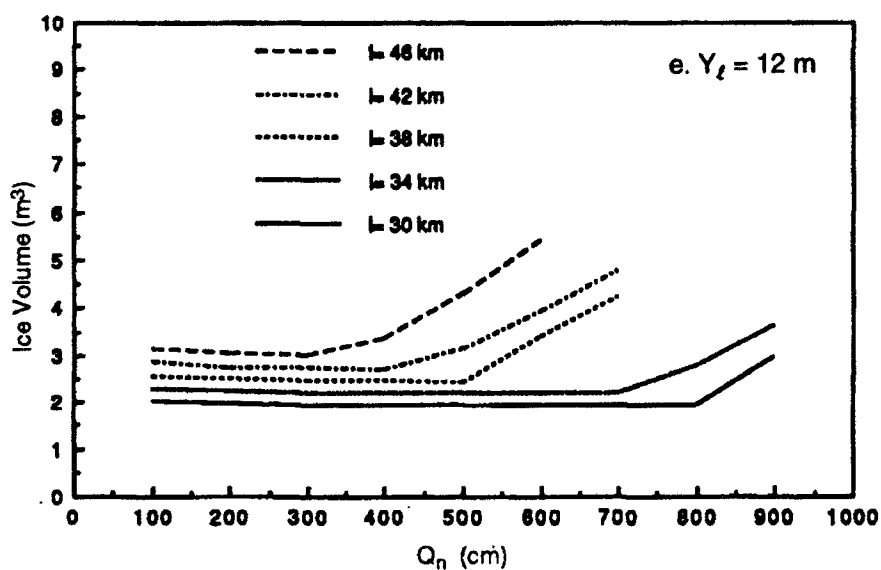
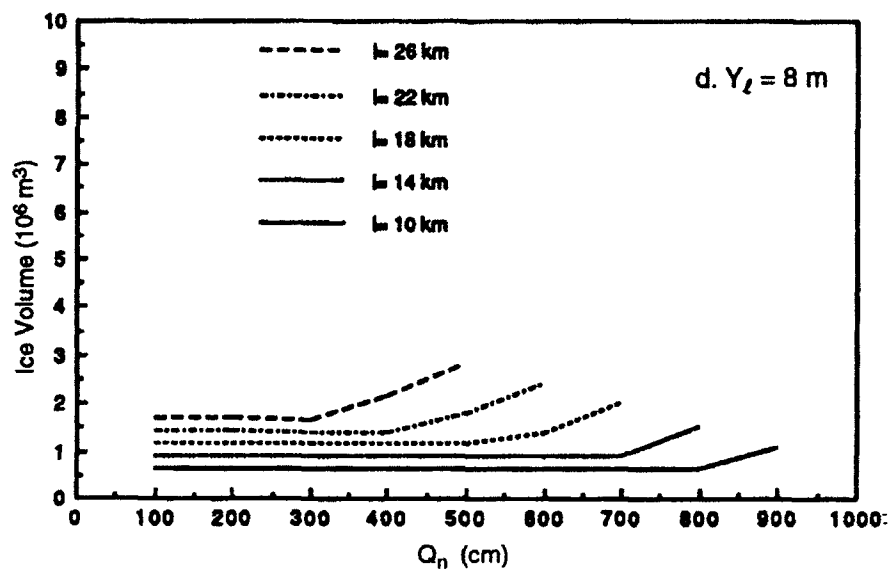


Figure 20 (cont'd). Volume of ice in ice cover for $S_0 = 2 \times 10^{-4}$, $T_a = -20^\circ\text{C}$.

cover stability. The influences on Q_0 of air temperature, however, remain a matter of speculation as they are not yet generally documented.

Values of Q_0 increase with increasing Y_L , decreasing S_0 , and decreasing ℓ , as one would expect. In addition, Q_0 is very sensitive to downstream depths; for example, Q_0 for a pool length of 50 km and channel slope of 2×10^{-4} increases from 150 to 520 m^3/s (5,300 to 18,360 ft^3/s), for a change in Y_L from 12 to 14 m. If, during a period of ice-cover formation, it is permissible to increase Y_L , significantly higher flows could be used to form frazil-generated ice covers for reduced periods, t_A . Also keep in mind that lesser values of t_A would be needed for ice covers to form over portions of, rather than entire, pool lengths.

The present study indicates that flow regulation (primarily discharge regulation) is a feasible approach to controlling ice-cover formation on pools of the upper Ohio River.

CONCLUSIONS AND RECOMMENDATIONS

To minimize frazil ice generation and thereby prevent the occurrence of deleterious frazil-ice-generated jams in rivers, rapid ice-cover formation is required. One way to achieve this is by means of flow regulation, especially discharge regulation. A numerical model is developed to simulate ice-cover formation by frazil-ice accumulation. The simulation model is applied to determine the time required to form accumulation ice covers

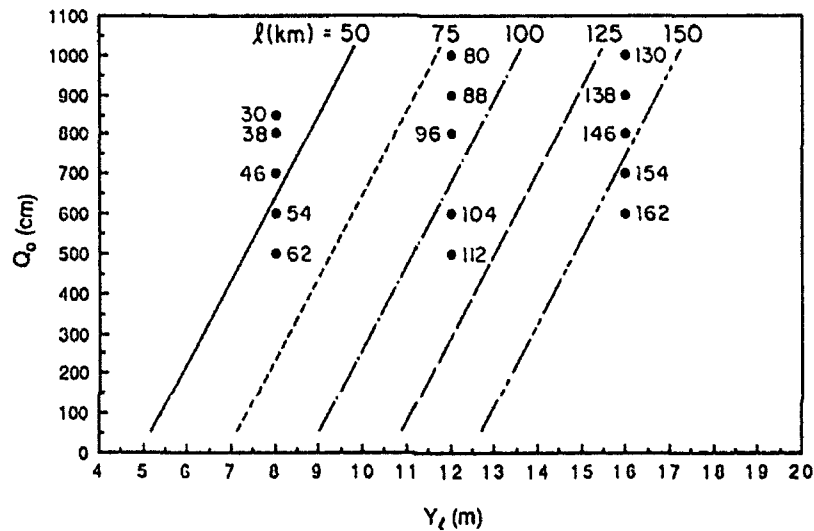


Figure 21. Optimal river discharge for $S_0 = 8 \times 10^{-5}$.

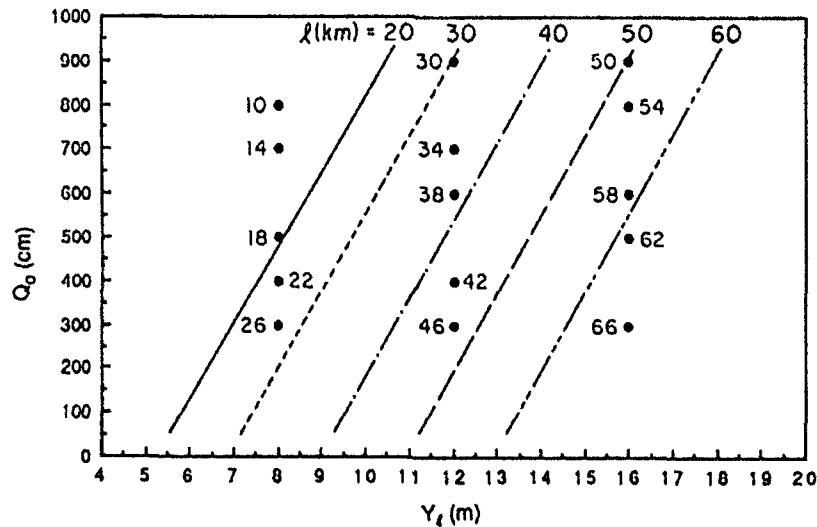


Figure 22. Optimal river discharge for $S_0 = 2 \times 10^{-4}$.

over individual river pools that are stage-regulated. The numerical results of the simulation model indicate that, for individual pools or reaches, there exists an optimal flow discharge that corresponds to a minimum time required for the ice cover to form. Optimal discharge increases with increasing downstream depth of flow, decreasing pool/reach length, and decreasing channel slope. In addition, time to form an ice cover decreases with decreasing air temperature. Figures 19 through 22 give information on times and ice volumes associated with ice-cover formation over several sets of pool/reach bed slope, length, and downstream depth.

Based on an example involving two pools of the Ohio River, at Hannibal and Montgomery, it appears feasible to minimize the amount of frazil ice generation using existing navigation dams, which would serve as ice retention structures and flow-stage regulators, and existing flood-control reservoirs on tributaries that could be used to regulate flow discharge. The Ohio River and its principal tributaries, the Allegheny and the Monongahela rivers, however, comprise a fairly complex system of several pools, not just a single pool. Therefore it is of interest to minimize frazil ice growth and time for cover formation over extensive portions of the Ohio River; at least, over several pools, especially in the vicinity of potential problem locations. In this regard, the problem of controlled ice-cover formation is more complex for the Ohio River than it is for the St. Lawrence and Lule River examples cited in Section 2, *Control of River Ice Formation*. To minimize frazil ice growth in large portions of the Ohio River, it is necessary to treat the Ohio as a flow system such as indicated in Figure 6. It is beyond the scope of this study to provide a detailed guide as to how flow should be modified or regulated along the entire Ohio River. That task is a logical next step in fully determining the feasibility of flow regulation to control ice-cover formation on the Ohio. It would require a detailed flow model that simulates a series of pools, major tributaries, and linked flood-control reservoirs.

An additional logical next step would be to conduct a field experiment aimed at verifying the proposed strategy of flow regulation for ice management. The experiment should focus on a single pool. A reach on the Allegheny River below Kinzua Dam, where discharge could be controlled closely and shore ice as well as ice-cover formation could be monitored in detail, is recommended as a possible site for the field experiment. Information gained from such a field experiment would be useful in further development of a simulation model. In particular, it would provide substantial information on the genesis of frazil ice and stability criteria for ice-cover progression, important two- and three-dimensional effects not accounted for in the present one-dimensional simulation.

Further, in forming accumulation ice covers over critical pools, consideration should be given to passing to downstream pools ice formed on upstream pools. In this manner, periods required for ice-cover formation might be reduced. This consideration touches on an issue frequently confronting operators of lock and dam installations: whether or not to pass broken ice conveyed by the river. This issue has to be addressed in the context of coordinated efforts to either form or release ice covers so that damaging ice jams do not form.

LITERATURE CITED

- Aleinikov, S.M. and V.A. Korenkov (1972) Ice-cutting operations in river ice control. *Proceedings of IAHR/PIANC Symposium on River and Ice, Budapest, Hungary*, 6(B): 109-116.
- Ashton, G.D. (Ed.) (1986) *River and Lake Ice Engineering*, Water Resources Publications, Littleton, Colorado.
- Billfalk, L. (1984) Strategic hydro-power operation at freeze-up reduces ice jamming. *Proceedings of IAHR Symposium on Ice, Hamburg, West Germany*, 1: 255-264.
- Brocard, D.N. and D.R.F. Harlemann (1976) One-dimensional temperature predictions in unsteady flows. *Journal of the Hydraulics Division, ASCE*, March, 102(HY3): 227-240.
- Cunge, J.A. and N. Perdreau (1973) Mobile Bed Fluvial Mathematical Models. *La Houille Blanche, Grenoble, France*, 28(7): 561-580.
- Cunge, J.A., F.M. Holly Jr. and A. Verwey (1980) Practical aspects of computational river hydraulics. Iowa Institute of Hydraulic Research, Iowa City, Iowa.
- Daly, S.F. (1984a) Frazil ice dynamics. USA Cold Regions Research and Engineering Laboratory, Monograph 84-1.
- Daly, S.F. (1984b) Winter environment of the Ohio River Valley. USA Cold Regions Research and Engineering Laboratory, unpublished report.
- Deck, D. (1984) Controlling river ice to alleviate ice jam flooding. *Proceedings of IAHR Symposium on Ice, Hamburg, West Germany*, 3: 69-76.
- Deck, D. and G. Gooch (1984) Performance of the Allegheny River ice control structure, 1983. USA Cold Regions Research and Engineering Laboratory, Special Report 84-13.
- Ettema, R., Karim, M.F. and J.F. Kennedy (1984) Frazil ice formation. USA Cold Regions Research and Engineering Laboratory, Report 84-18.
- Foltyn, E.P. (1986) Laboratory and field tests of a wire mesh frazil collector. *Proceedings of Fourth Workshop on Hydraulics of River Ice, Montreal*, June 19-20.
- Gatto, L., S.F. Daly and K. Carey (1986) Ice atlas, 1984-1985: Ohio River, Allegheny River, Mononga-

- hela River. USA Cold Regions Research and Engineering Laboratory, Special Report 86-23.
- Holly Jr., F.M. and A. Preissmann** (1977) Accurate calculation of transport in two dimensions. *Journal of the Hydraulics Division, ASCE*, November, Vol. 103, No. HY11.
- IAHR, Working Group on River Ice Hydraulics** (1986) River ice jams: A state-of-the-art report. *Proceedings of the IAHR Symposium on Ice, Iowa City, Iowa*, 3: 561–594.
- Jensen, M.** (1981) Ice problems of Vittjarv power plant—Measures and results. *Proceedings of the IAHR Symposium on Ice, Quebec, Canada*, 1: 238–251.
- Kivisild, H.R.** (1959) Hydrodynamic analysis of ice floods. *Proceedings of the Eighth Congress of IAHR, Montreal, Canada*, vol. 2, paper 23F.
- Lawrie, C.J.R.** (1972) Ice control measures on the St. Lawrence River. *Proceedings of the 29th Annual Eastern Snow Conference, Oswego, N.Y.*, p. 123–146.
- Martin, S.** (1981) Frazil ice in rivers and oceans. *Annual Review of Fluid Mechanics*, 13: 379–397.
- Michel, B.** (1971) Winter regime of rivers and lakes. USA Cold Regions Research and Engineering Laboratory, Monograph III-B1a.
- Michel, B.** (1978) Ice accumulation at freeze-up or break-up. *Proceedings of the Symposium on Ice Problems, IAHR, Luleå, Sweden*, 2: 301–317.
- ORDIC** (1978) Closure report. USA Corps of Engineers, Ohio River Division Ice Committee, 20 February.
- Osterkamp, T.E.** (1978) Frazil ice formation: A review. *Journal of the Hydraulics Division, ASCE*, 104(9): 1239–1255.
- Pariset, E., R. Hausser and A. Gagnon** (1966) Formation of ice covers and ice jams in rivers. *Journal of the Hydraulics Division, ASCE*, 92(6): 4965–4989.
- Park, C. and R.C. Gerard** (1984) Hydraulic characteristics of frazil floes—Some preliminary experiments. *Proceedings of the IAHR Symposium on Ice, Hamburg, West Germany*, 3: 27–36.
- Perham, R.** (1981) Tests of frazil collector lines to assist ice cover formation. *Canadian Journal of Civil Engineering*, 8: 442–448.
- Perham, R.** (1983) Ice retention structures. USA Cold Regions Research and Engineering Laboratory, Report 83-30.
- Perham, R.** (1986) Preliminary study of a structure to form an ice cover on river rapids during winter. *Proceedings of the IAHR Symposium on Ice, Iowa City, Iowa*, 1: 439–450.
- Petkovic, S., R. Pavlovic and S. Varga** (1984) Concept and experience in controlling the ice regime on the Yugoslav reach of the Danube after the construction of the Iron Gate Dam. *Proceedings of the IAHR Symposium on Ice, Hamburg, West Germany*, 1: 291–302.
- Rozsnyoi, P.** (1972) Activity for the prevention of ice damage in Hungary. *Proceedings of the IAHR/PIANC Symposium on Rivers and Ice, Budapest, Hungary*, 6(B): 41–48.
- Shen, H.T., and L.A. Chiang** (1984) Simulation of growth and decay of river ice cover. *Journal of Hydraulic Engineering, ASCE*, 110(7): 958–971.
- Shen, H.T. and C.F. Ho** (1986) Two-dimensional simulation of ice cover formation in a large river. *Proceedings of the IAHR Symposium on Ice, Iowa City, Iowa*, 1: 547–558.
- Shen, H.T., R.W. Ruggles and G.B. Batson** (1984) Field investigation of St. Lawrence River hanging ice dams, winter of 1983–84. U.S. Department of Transportation, Washington, D.C. Report DTSL55-84-C-C0085A, p. 85.
- Uzuner, M.S.** (1975) The composite roughness of ice covered streams. *Journal of Hydraulic Research*, 13(1): 79–101.
- Uzuner, M. and J.F. Kennedy** (1972) Stability of floating ice blocks. *Journal of the Hydraulics Division, ASCE*, 98(HYR): 2117–1383.
- Wigle, T.E., J. Bartholomew, and C.J.R. Lawrie** (1981) Winter operations: International section of the St. Lawrence River. *Proceedings of the IAHR International Symposium on Ice, Quebec City*, p. 193–202.
- Wuebben, J.** (1984) The rise pattern and velocity of frazil ice. *Proceedings of Workshop on Hydraulics of River Ice, Fredericton, June 20–21*, p. 297–316.
- Zufelt, J.E. and D. Calkins** (1985) Survey of ice problems in navigable waterways. USA Cold Regions Research and Engineering Laboratory, Special Report 85-2.

APPENDIX A: EXPRESSIONS FOR COEFFICIENTS

The coefficients a_i, b_i, \dots , in eq 10 and a_f, b_f, \dots , in eq 11 are given below:

$$a_i = \frac{1}{2\Delta t} B_{i+1}, \quad b_i = \frac{\theta}{\Delta x}$$

$$c_i = \frac{-1}{2\Delta t} B_i, \quad d_i = \frac{\theta}{\Delta x}, \quad \text{and } e_i = \frac{-1}{\Delta x} (Q_{i+1} - Q_i)$$

$$\begin{aligned} a_f = & -\frac{\alpha\theta}{\Delta x} (Q_{i+1} - Q_i) \left(\frac{Q}{A^2} \right)_{i+1} B_{i+1} \\ & - \frac{\alpha\theta}{4\Delta x} \left[\left(\frac{Q}{A} \right)_{i+1} + \left(\frac{Q}{A} \right)_i \right] \left[\left(\frac{Q}{A} \right)_{i+1} + \left(\frac{Q}{A} \right)_i - 2(A_{i+1} - A_i) \left(\frac{Q}{A^2} \right)_{i+1} \right] B_{i+1} \\ & + \frac{g\theta}{2\Delta x} [(y_{i+1} - y_i) B_{i+1} + (A_{i+1} + A_i)] \\ & + \frac{g\theta}{2} \left\{ [\beta S_{fi} + (1 - \beta) S_{fi+1}] B_{i+1} - (A_{i+1} + A_i) \left(\frac{2(1 - \beta) Q |Q|}{K^3} K' \right)_{i+1} \right\} \\ & + \frac{g\theta}{2\Delta x} (\bar{\eta}_{i+1} - \bar{\eta}_i) B_{i+1} \end{aligned}$$

$$\begin{aligned} b_f = & \frac{1}{2\Delta t} + \frac{\alpha\theta}{\Delta x} \left[\left(\frac{Q}{A} \right)_{i+1} + \left(\frac{Q}{A} \right)_i + \frac{Q_{i+1} - Q_i}{A_{i+1}} \right] \\ & - \frac{\alpha\theta}{2\Delta x} \left[\left(\frac{Q}{A} \right)_{i+1} + \left(\frac{Q}{A} \right)_i \right] (A_{i+1} - A_i) \frac{1}{A_{i+1}} \\ & + \frac{g\theta}{2} (A_{i+1} + A_i) \left(\frac{2(1 - \beta) |Q|}{K^2} \right)_{i+1} \end{aligned}$$

$$\begin{aligned} c_f = & \frac{\alpha\theta}{\Delta x} (Q_{i+1} - Q_i) \left(\frac{Q}{A^2} \right)_i B_i \\ & - \frac{\alpha\theta}{4\Delta x} \left[\left(\frac{Q}{A} \right)_{i+1} + \left(\frac{Q}{A} \right)_i \right] \left[\left(\frac{Q}{A} \right)_{i+1} + \left(\frac{Q}{A} \right)_i + 2(A_{i+1} - A_i) \left(\frac{Q}{A^2} \right)_i \right] B_i \\ & - \frac{g\theta}{2\Delta x} [(y_{i+1} - y_i) B_i - (A_{i+1} + A_i)] \\ & - \frac{g\theta}{2} \left\{ [\beta S_{fi} + (1 - \beta) S_{fi+1}] B_i - (A_{i+1} + A_i) \left(\frac{2\beta Q |Q|}{K^3} K' \right)_i \right\} \\ & - \frac{g\theta}{2\Delta x} (\bar{\eta}_{i+1} - \bar{\eta}_i) B_i \end{aligned}$$

$$d_f = -\frac{1}{2\Delta t} + \frac{\alpha\theta}{\Delta x} \left[\left(\frac{Q}{A} \right)_{i+1} + \left(\frac{Q}{A} \right)_i - \frac{Q_{i+1} - Q_i}{A_i} \right]$$

$$\begin{aligned}
& + \frac{\alpha \theta}{2\Delta x} \left[\left(\frac{Q}{A} \right)_{i+1} + \left(\frac{Q}{A} \right)_i \right] (A_{i+1} - A_i) \frac{1}{A_i} \\
& - \frac{g\theta}{2} (A_{i+1} + A_i) \left(\frac{2\beta|Q|}{K^2} \right)_i
\end{aligned}$$

and

$$\begin{aligned}
e_f = & - \frac{\alpha}{\Delta x} \left[\left(\frac{Q}{A} \right)_{i+1} + \left(\frac{Q}{A} \right)_i \right] (Q_{i+1} - Q_i) \\
& + \frac{\alpha}{4\Delta x} \left[\left(\frac{Q}{A} \right)_{i+1} + \left(\frac{Q}{A} \right)_i \right]^2 (A_{i+1} - A_i) \\
& - \frac{g}{2\Delta x} (A_{i+1} + A_i) (y_{i+1} - y_i) \\
& - \frac{g}{2} (A_{i+1} + A_i) [\beta S_{fi} + (1 - \beta) S_{fi+1}] \\
& - \frac{g}{2\Delta x} (A_{i+1} + A_i) (\bar{\eta}_{i+1} - \bar{\eta}_i)
\end{aligned}$$

where $K = \frac{1}{n} AR^{2/3}$ and $K' = \frac{dk}{dy}$.

APPENDIX B: LISTING OF COMPUTER PROGRAM

```

C
C   SIMULATION OF THE ICE GENERATION IN AN UNSTEADY OPEN CHANNEL
C   SYSTEM.
C
C   This program can handle a system of open channels with
C   weirs, storage ponds.
C   Currently this program can handle only one node point with several
C   branched channels but it can be easily modified to handle a system
C   with several node points.
C   Looped channels are not considered in this program.
C
C   All channel informations should be given in order of
C   computational sequence, i.e.,
C
C   U/S of channel 1. -----> Node point
C   U/S of channel 2. -----> Node point
C   ----->
C   ----->
C   U/S of channel n. -----> Node point
C   Node point -----> D/S of main channel
C
C   COMMON /C01/ A(34),B(34),BW(34),H(34),R(34),S(34),
C   #      CK(34),DKY(34),CKST(34),Z(34)
C   COMMON /C02/ Q(34),V(34),Y(34)
C   COMMON /C03/ E(34),F(34),ITYP(34)
C   COMMON /C04/ YTDB(30),QTDB(30),QDB(30),YDB(30),NQDB,NYDB
C   COMMON /C05/ QTUB(10,2),QUB(10,2),NQUB(2),NCHAN
C   COMMON /C06/ N,NT,TIME,I,KI,MNT1,LE
C   COMMON /C07/ DELY
C   COMMON /C08/ SO,ZL,ZR,DPY
C   COMMON /C09/ GRAV,SWI,DELTAT,ALPHA,BETA,THETA
C   COMMON /C10/ NNOD,NOD(2),NOD1(2)
C   COMMON /C11/ WY,WB,CMU
C   COMMON /C13/ DELX(34),X(34)
C   COMMON /C14/ SURF,YBASE
C   COMMON /C15/ ICEFLG(34),T(34),C(34),IH(34)
C
C   Following are the key variables of this program.
C
C   A(I): area of the cross section.
C   B(I): width of the cross section at the top.
C   BW(I): width of the cross section at the bottom.
C   CKST(I): Strickler's coefficient.
C   CMU: weir coefficient.
C   DELY: dy.
C   DPY: dp/dy.
C   H(I): water depth.
C   P: wetted perimeter.
C   R(I): hydraulic radius.
C   S(I): energy slope.
C   Q(I): water discharge.
C   V(I): velocity.
C   Y(I): water surface elevation from the datum.
C   E(I): coefficient E.
C   F(I): coefficient F.
C   YTDB(K): time at which the D/S water surface level is given.
C   QTDB(K): time at which the D/S water discharge is given.
C   YDB(K): given D/S water surface level.
C   QTB(K): given D/S water discharge.
C   NQDB: number of discharge data for the D/S boundary condition.

```



```

C      NYDB: number of stage data for the D/S boundary condition.
C      QTUB(K): time at which the U/S discharge is given.
C      QUB(K): given U/S discharge.
C      NQUB: number of discharge hydrograph data for the U/S B.C.
C      MNT: number of time steps for computation.
C      NST: number of time steps for stabilization.
C      ICEFLG: flag for ice cover. no ice = 0, ice covered = 1.
C      N: number of space intervals.
C      NCHAN: number of channels branched from a node point.
C      NNOD: same as NCHAN.
C      NOD(K): point No. of junction point of Kth channel.
C      NOD1(K): point No. of node point connected to current junction
C              point.
C      NT: time index.
C      TIME: elapsed time from the starting.
C      SO: bed slope.
C      ZL: slope of the left bank.
C      ZR: slope of the right bank.
C      WY: level of a weir.
C      WB: width of a weir.
C      SURF: surface area of a storage pond.
C      YBASE: base level of a storage pond.
C
C      ITYP=1 : 1-D point
C              2 : U/S point,  $Q=Q(t)$ 
C              3 : storage pond
C              4 : junction point
C              5 : weir
C              6 : D/S point,  $Q=Q(y)$ 
C              7 : D/S point,  $Q=Q(t)$ 
C              8 : D/S point,  $y=y(t)$ 
C
C

```

```

C      DIMENSION TYPE(8),PNAME(34),NAME(34),XO(34)
C      DIMENSION HYDRO(28,200),FRONT(200),VOLICE(200)
C      DIMENSION IQHYD(10),IYHYD(10),ITHYD(10),ICHYD(10),IZHYD(10)
C      DIMENSION TPT(30),ZNAME(1),KNAME(2)
C      NCHAN=0
C      NQDB=0
C      NYDB=0
C      NNOD=0
C      READ(1,*) N,NOPT
C      IF(NOPT.EQ. 0) GO TO 810
C      READ(1,*) GQ,GY,GS,GDELX,GBW,GCKST
C      X(1)=0.0
C      Z(N)=0.0
C      Y(N)=GY
C      DZ=GDELX*1000.*GS
C      HO=(GQ/(GCKST*GBW*GS**0.5))**0.6
C      DO 800 I=1,N
C      ITYP(I)=1
C      DELX(I)=GDELX
C      BW(I)=GBW
C      CKST(I)=GCKST
C      Q(I)=GQ
C      IF(I.EQ. N) GO TO 800
C      X(I+1)=X(I)+DELX(I)
C      Z(N-I)=Z(N-I+1)+DZ
C      Y(N-I)=Z(N-I)+HO
C      IF(Y(N-I).LT. GY) Y(N-I)=GY
C 800 CONTINUE
C 810 DO 10 I=1,N
C      READ(1,*) PNAME(I),ITYP(I),X(I),DELX(I),Z(I),BW(I),CKST(I)
C      ZNAME(1)=PNAME(I)
C      DECODE(1,700,ZNAME) NAME(I)
C      WRITE(6,610) I,PNAME(I),ITYP(I),X(I),DELX(I),Z(I),BW(I),CKST(I)
C      DELX(I)=DELX(I)*1000.0
C      XO(I)=X(I)

```

```

      X(I)=X(I)*1000.0
      GO TO (11,2,3,4,5,6,6,6), ITYP(I)
C
C      U/S of a channel : input discharge hydrograph is required as
C      the boundary condition.
C
      2 NCHAN=NCHAN+1
      KNAME(NCHAN)=NAME(I)
      READ(1,*) NQ,(QTUB(J,NCHAN),QUB(J,NCHAN),J=1,NQ)
      NQUB(NCHAN)=NQ
      WRITE(6,615) (QTUB(J,NCHAN),QUB(J,NCHAN),J=1,NQ)
      GO TO 11
C
C      Storage pond : surface area in hectare and base level are
C      required.
C
      3 READ(1,*) SURF,YBASE
      WRITE(6,620) SURF,YBASE
      SURF=SURF*10000.0
      GO TO 10
      4 NNOD=NNOD+1
      NOD(NNOD)=I
      READ(1,*) NOD1(NNOD)
      WRITE(6,630) NOD1(NNOD)
      GO TO 10
C
C      Weir : weir elevation, width, and weir coefficient are required.
C
      5 READ(1,*) WY,WB,CMU
      WRITE(6,640) WY,WB,CMU
      GO TO 10
      6 IF(ITYP(I)-7) 7,8,9
C
C      D/S B.C. : Rating curve :  $Q=Q(y)$ 
C
      7 WRITE(6,650)
      GO TO 10
C
C      D/S B.C. :  $Q=Q(t)$ 
C
      8 READ(1,*) NQDB,(QTDB(J),QDB(J),J=1,NQDB)
      WRITE(6,660) (QTDB(J),QDB(J),J=1,NQDB)
      GO TO 10
C
C      D/S B.C. :  $y=y(t)$ 
C
      9 READ(1,*) NYDB,(YTDB(J),YDB(J),J=1,NYDB)
      WRITE(6,670) (YTDB(J),YDB(J),J=1,NYDB)
      GO TO 10
      11 CONTINUE
      10 CONTINUE
C
C      INITIALIZE THE VARIABLES AND READ INITIAL CONDITIONS
C
      SO=(Z(N-1)-Z(N))/DELX(N-1)
      IF(NOPT.EQ. 0) READ(1,*) (Y(I),Q(I),I=1,N)
      READ(1,*) GRAV,ALPHA,BETA,THETA
      READ(1,*) TYPE,ZL,ZR
      READ(1,*) TMAX,DELT,NST
      DELTAT=DELT*60.0
      MNT=TMAX*60.0/DELTAT+0.01
      MNT1=MNT+1
      NTT=MNT+NST
C
C      READ TIMES FOR SURFACE PROFILE.
C
      READ(1,*) NIPT,(TPT(J),J=1,NIPT)

```

```

C
C   READ SECTION NO. FOR HYDROGRAPH.
C
  READ(1,*) NQHYD,(IQHYD(I),I=1,NQHYD)
  READ(1,*) NYHYD,(IYHYD(I),I=1,NYHYD)
  READ(1,*) NTHYD,(ITHYD(I),I=1,NTHYD)
  READ(1,*) NCHYD,(ICHYD(I),I=1,NCHYD)
  READ(1,*) NZHYD,(IZHYD(I),I=1,NZHYD)

  NQL=NQHYD+1
  NYF=NQL+1
  NYL=NQL+NYHYD
  NTF=NYL+1
  NTL=NTF+NTHYD
  NCF=NTL+1
  NCL=NTL+NCHYD
  NZF=NCL+1
  NZL=NCL+NZHYD

C
C   PRINT INITIAL VALUES
C
  WRITE(6,200) N,NCHAN,GRAV,TYPE,SO,ZL,ZR,TMAX,DELTAT,
#           MNT,NST,ALPHA,BETA,THETA

C
C   BEGIN LOOP FOR TIME
C
  TIME=0.0
  NT=1
  CALL THICON
25 DO 30 I=1,N
30 H(I)=Y(I)-Z(I)
  KT=NT-NST+1
  CALL ICE
  CALL SECTN
  DO 40 I=1,N
40 V(I)=Q(I)/A(I)
  IF(NT .LT. NST) GO TO 46

C
C   COMPUTE TEMPERATURE DISTRIBUTION AND ICE CONCENTRATION.
C
  CALL TEMP
  CALL ICECVR
  CALL CONDC
  IF(TH(N) .GT. 0.0) GO TO 35
  FRONT(KT)=0.0
  VOLICE(KT)=0.0
  GO TO 38
35 SUMICE=0.0
  N1=N-1
  DO 36 I=1,N1
  NI=N-I
  IF(TH(NI) .LE. 0.0) GO TO 37
  SUMICE=SUMICE+TH(NI)*DELX(NI)*B(NI)
36 CONTINUE
37 VOLICE(KT)=SUMICE
  FRONT(KT)=(X(N)-X(NI+1))/1000.

C
C   CREATE OUTPUT FILE
C
38 HYDRO(1,KT)=TIME/60.0

  DO 41 J=1,NQHYD
41 HYDRO(J+1,KT)=Q(IQHYD(J))
  DO 42 J=1,NYHYD
42 HYDRO(J+NQL,KT)=Y(IYHYD(J))
  DO 43 J=1,NTHYD
43 HYDRO(J+NYL,KT)=T(ITHYD(J))
  DO 44 J=1,NCHYD

```

```

44 HYDRO(J+NTL,KT)=C(ICHYD(J))
   DO 45 J=1,NZHYD
45 HYDRO(J+NCL,KT)=TH(IZHYD(J))
46 DO 49 J=1,NIPT
   IF(ABS(TIME-TPT(J)) .GT. 1.E-2 .OR. NT .LT. NST) GO TO 49
   WRITE(6,300) TIME
   DO 48 K=1,NCHAN
   WRITE(6,310) K
   DO 47 I=1,N
   IF(NAME(I) .NE. KNAME(K)) GO TO 47
   WRITE(6,320) I,PNAME(I),XO(I),Y(I),H(I),A(I),Q(I),T(I),C(I),TH(I)
47 CONTINUE
48 CONTINUE
49 CONTINUE
   IF(NT .GE. NTT) GO TO 100
   IF(NT .LT. NST) GO TO 50
   TIME=TIME+DELT
50 CALL DSWEET
   NT=NT+1
   GO TO 25
100 WRITE(6,500) (PNAME(IQHYD(J)),J=1,NQHYD)
   DO 110 J=1,MNT1
110 WRITE(6,510) HYDRO(1,J),(HYDRO(1,J),I=2,NQL)
   WRITE(6,520) (PNAME(IYHYD(J)),J=1,NYHYD)
   DO 120 J=1,MNT1
120 WRITE(6,510) HYDRO(1,J),(HYDRO(1,J),I=NYF,NYL)
   WRITE(6,530) (PNAME(ITHYD(J)),J=1,NTHYD)
   DO 130 J=1,MNT1
130 WRITE(6,512) HYDRO(1,J),(HYDRO(1,J),I=NTF,NTL)
   WRITE(6,540) (PNAME(ICHYD(J)),J=1,NCHYD)
   DO 140 J=1,MNT1
140 WRITE(6,511) HYDRO(1,J),(HYDRO(1,J),I=NCF,NCL)
   WRITE(6,550) (PNAME(IZHYD(J)),J=1,NZHYD)
   DO 150 J=1,MNT1
150 WRITE(6,512) HYDRO(1,J),(HYDRO(1,J),I=NZF,NZL)
   WRITE(6,560)
   WRITE(6,513) (HYDRO(1,J),FRONT(J),VOLICE(J),J=1,MNT1)
   STOP
200 FORMAT(1H1,/,5X,'***** P R O B L E M   D E S C R I P T I O N **
#*****',/,/, ' < GEOMETRICAL CONDITION >',/,/,
# ' Number of points = ',I3,/
# ' Number of channels = ',I3,/
# ' Gravitational acceleration = ',F5.2,'(m/sec**2)',/
# ' Channel type = ',8A4,/
# ' Bed slope at D/S = ',F8.6,/
# ' Slope of left bank = 1 : ',F3.1,/
# ' Slope of right bank = 1 : ',F3.1,/,/,
# ' < NUMERICAL CONDITION >',/,/,
# ' Maximum time = ',F7.1,'(min)',/
# ' Time step = ',F7.1,'(sec)',/
# ' No. of time step for unsteady flow = ',I3,/
# ' No. of time step for stabilization = ',I3,/
# ' Energy correction coefficient = ',F3.1,/
# ' Weighting coefficient in space = ',F4.2,/
# ' Weighting coefficient in time = ',F4.2,/,/,
300 FORMAT(1H1,/,/, ' Time = ',F7.1,'(min)')
310 FORMAT(//,10X,'Channel No. = ',I2,/,/
# 2X,'No. Name X(km) Y(m) h(m) A(m**2) Q(cms)'
# , ' TEMP(C) C(X) ICE(m)',/,/)
320 FORMAT(14,3X,A4,F6.1,F8.3,F7.3,F8.2,F8.2,F9.4,2PF7.3,OPF8.4)
500 FORMAT(1H1,/,5X,'< D I S C H A R G E   H Y D R O G R A P H >'
# ,/,14X,'Water Discharge (cms)',/,/
# ,3X,'TIME',4X,10(A4,5X),/,/)
510 FORMAT(1X,F6.2,10F9.3)
511 FORMAT(1X,OPF6.2,2P10F9.3)
512 FORMAT(1X,F6.2,10F9.4)
513 FORMAT(1X,F6.2,F10.2,F12.0)

```

```

520 FORMAT(1H1,/,5X,'< S T A G E   H Y D R O G R A P H >',//
#       ,14X,'Water Surface Level (m)',//
#       ,3X,'TIME',4X,10(A4,5X),//)
530 FORMAT(1H1,/,5X,'< T E M P E R A T U R E   D I S T R >',//
#       ,14X,'Average temperature (C)',//
#       ,3X,'TIME',4X,10(A4,5X),//)
540 FORMAT(1H1,/,5X,'< I C E   C O N C E N T R A T I O N >',//
#       ,14X,'Average concentration (%)',//
#       ,3X,'TIME',4X,10(A4,5X),//)
550 FORMAT(1H1,/,5X,'< I C E   T H I C K N E S S >',//
#       ,14X,'Ice cover thickness (m)',//
#       ,3X,'TIME',4X,10(A4,5X),//)
560 FORMAT(1H1,/,5X,'< I C E   A C C U M U L A T I O N >',//
#       ,3X,'TIME',4X,'X (km)',3X,'VOL (m**3)',//)
610 FORMAT(/,1X,60('-'),/,1X,'No. ',I2,2X,A4,2X,'Type=',I2,2X
#       ,X='F4.1,2X,'DX='F4.1,2X,'Z='F5.2,2X,'BW='F5.1
#       ,2X,'Kst='F4.1,/,1X,60('-'))
615 FORMAT(/,5X,'< U P S T R E A M   B O U N D A R Y   P O I N T >',//
#       ,5X,'*** Input Hydrograph ***',//
#       ,X='T(min) Q(cms)',/(F11.3,5X,F11.3))
620 FORMAT(/,5X,'< S T O R A G E   P O N D >',//
#       ,5X,'Surface Area = ',F4.1,'(ha)',/
#       ,5X,'Bottom Elevation = ',F5.2,'(m)')
630 FORMAT(/,5X,'< J U N C T I O N   P O I N T >',//
#       ,5X,'D/S point = No.',I2)
640 FORMAT(/,5X,'< R E C T A N G U L A R   W E I R >',//
#       ,5X,'Elevation of the Weir = ',F4.1,'(m)',/
#       ,5X,'Width of the Weir = ',F4.1,'(m)',/
#       ,5X,'Weir Coefficient = ',F4.1)
650 FORMAT(/,5X,'< D / S   B O U N D A R Y   P O I N T >',//
#       ,5X,'*** Rating Curve ***')
660 FORMAT(/,5X,'< D / S   B O U N D A R Y   P O I N T >',//
#       ,5X,'*** Discharge Hydrograph ***',//
#       ,X='T(min) Q(cms)',/(F11.3,5X,F11.3))
670 FORMAT(/,5X,'< D / S   B O U N D A R Y   P O I N T >',//
#       ,5X,'*** Stage Hydrograph ***',//
#       ,X='T(min) Y(m)',/(F11.3,5X,F11.3))
700 FORMAT(A1)
      END

```

```

      SUBROUTINE DSWEET
      COMMON /C01/ A(34),B(34),BW(34),H(34),R(34),S(34),
#       CK(34),DKY(34),CKST(34),Z(34)
      COMMON /C02/ Q(34),V(34),Y(34)
      COMMON /C03/ E(34),F(34),ITYP(34)
      COMMON /C06/ N,NT,TIME,I,KT,MNT1,LE
      COMMON /C07/ DELY
      COMMON /C09/ GRAV,SWI,DELTAT,ALPHA,BETA,THETA
      COMMON /C10/ NNOD,NOD(2),NOD1(2)
      COMMON /C12/ AA,BB,CC,DD,GG,AA1,BB1,CC1,DD1,GG1
      COMMON /C13/ DELX(34),X(34)
      COMMON /C15/ ICEFLG(34),T(34),C(34),TH(34)
      DIMENSION CL(34),CM(34),CN(34)
      IF(NT.GT. 1) GO TO 5
      G2=GRAV*0.5
      GT=GRAV*THETA
      GT2=GT*0.5
      R2T=0.5/DELTAT
      N1=N-1
      DO 100 I=1,N1
      DELTAX=DELX(I)
      GO TO (10,20,30,40,50), ITYP(I)
      20 CALL UPBC
      GO TO 60

```

```

30 CALL POND
   GO TO 90
40 CALL JUNC
   GO TO 100
50 CALL WEIR
   GO TO 90
10 IF(DELTA .EQ. DELX(I-1)) GO TO 70
60 ADX=ALPHA/DELTA
   A4DX=ADX*0.25
   ATDX=ADX*THETA
   AT2DX=ATDX*0.5
   AT4DX=AT2DX*0.5
   GT2DX=GT2/DELTA
   G2DX=G2/DELTA
70 QM=Q(I+1)-Q(I)
   VV=V(I+1)+V(I)
   AMA=A(I+1)-A(I)
   YMY=Y(I+1)-Y(I)
   TMT=(TH(I+1)-TH(I))*SWI
   APA=A(I+1)+A(I)
   SPS=BETA*S(I)+(1.-BETA)*S(I+1)
   QA1=V(I+1)/A(I+1)
   QA=V(I)/A(I)
C
C   COEFFICIENTS OF THE DYNAMIC EQUATION
C
   AA=-ATDX*QM*QA1*B(I+1)-AT4DX*VV*(VV-2.*AMA*QA1)*B(I+1)
   # +GT2DX*((YMY+TMT)*B(I+1)+APA)
   # +GT2*(SPS*B(I+1)-2.*APA*(1.-BETA)*S(I+1)/CK(I+1)*DKY(I+1))
   CC=ATDX*QM*QA*B(I)-AT4DX*VV*(VV+2.*AMA*QA)*B(I)
   # -GT2DX*((YMY+TMT)*B(I)-APA)
   # -GT2*(SPS*B(I)-2.*APA*BETA*S(I)/CK(I)*DKY(I))
   BB=R2T+ATDX*(VV+QM/A(I+1))-AT2DX*VV*AMA/A(I+1)
   # +GT*APA*(1.-BETA)*ABS(Q(I+1))/(CK(I+1)*CK(I+1))
   DD=-R2T+ATDX*(VV-QM/A(I))+AT2DX*VV*AMA/A(I)
   # -GT*APA*BETA*ABS(Q(I))/(CK(I)*CK(I))
   GG=-ADX*VV*QM+A4DX*VV*VV*AMA-G2DX*APA*(YMY+TMT)-G2*APA*SPS
C
C   COEFFICIENTS OF THE CONTINUITY EQUATION
C
   AA1=R2T*B(I+1)
   CC1=-R2T*B(I)
   BB1=THETA/DELTA
   DD1=BB1
   GG1=-QM/DELTA
C
90 CDCD=CC1*DD-CC*DD1
   CL(I)=(AA1*DD-AA*DD1)/CDCD
   CM(I)=(BB1*DD-BB*DD1)/CDCD
   CN(I)=(DD1*GG-DD*GG1)/CDCD
   CDE=CC1+DD1*E(I)
   BCC=BB1-CM(I)*CDE
   E(I+1)=(CL(I)*CDE-AA1)/BCC
   F(I+1)=(CN(I)*CDE+DD1*F(I)+GG1)/BCC
100 CONTINUE
   CALL DNBC
   DELQ=E(N)*DELY+F(N)
   Y(N)=Y(N)+DELY
   Q(N)=Q(N)+DELQ
   DO 200 J=1,N1
   I=N-J
   IF(IYP(I) .NE. 4) GO TO 160
C
C   JUNCTION POINT
C
   DO 150 K=1,NNOD
   IF(I .EQ. MOD(K)) GO TO 155

```

```

150 CONTINUE
155 DELY=Y(NOD1(K))-Y(I)
    GO TO 165
160 DELY=CL(I)*DELY+CM(I)*DELQ+CN(I)
165 Y(I)=Y(I)+DELY
    DELQ=E(I)*DELY+F(I)
200 Q(I)=Q(I)+DELQ
    RETURN
    END

```

```

SUBROUTINE SECTN
COMMON /C01/ A(34),B(34),BW(34),H(34),R(34),S(34),
#          CK(34),DKY(34),CKST(34),Z(34)
COMMON /C02/ Q(34),V(34),Y(34)
COMMON /C06/ N,NT,TIME,I,KT,MNT1,LE
COMMON /C08/ SO,ZL,ZR,DPY
COMMON /C15/ ICEFLG(34),T(34),C(34),TH(34)
IF(NT.GT. 1) GO TO 10
ZRL=ZR+ZL
SL=SQRT(1.0+ZL*ZL)
SR=SQRT(1.0+ZR*ZR)
DPY=SR+SL
10 DO 20 I=1,N
    B(I)=BW(I)+H(I)*ZRL
    A(I)=(BW(I)+B(I))*H(I)*0.5
    P=BW(I)+H(I)*DPY
    IF(ICEFLG(I).EQ. 1) P=P+B(I)
    R(I)=A(I)/P
    CKR23=CKST(I)*R(I)**0.6666667
    DKY(I)=0.6666667*CKR23*(2.5*B(I)-R(I)*DPY)
    CK(I)=CKR23*A(I)
20 S(I)=Q(I)*ABS(Q(I))/(CK(I)*CK(I))
    RETURN
    END

```

```

SUBROUTINE INBC
COMMON /C01/ A(34),B(34),BW(34),H(34),R(34),S(34),
#          CK(34),DKY(34),CKST(34),Z(34)
COMMON /C02/ Q(34),V(34),Y(34)
COMMON /C03/ E(34),F(34),ITYP(34)
COMMON /C04/ YTDB(30),QTDB(30),QDB(30),YDB(30),NQDB,NYDB
COMMON /C06/ N,NT,TIME,I,KT,MNT1,LE
COMMON /C07/ DELY
COMMON /C08/ SO,ZL,ZR,DPY

IF(NT.GT. 1) GO TO 5
CKS5=CKST(N)*SO**0.5
NQDB1=NQDB-1
NYDB1=NYDB-1
5 IF(ITYP(N)-7) 30,10,20

C
C   INTERPOLATE THE DISCHARGE HYDROGRAPH
C
10 IF(TIME.GE. QTDB(1)) GO TO 12
    DELY=(QDB(1)-Q(N)-F(N))/E(N)
    RETURN
12 DO 15 K=1,NQDB1
    IF(.NOT.(TIME.GE. QTDB(K).AND.
#       TIME.LT. QTDB(K+1))) GO TO 15
    DELY=(QDB(K)+(TIME-QTDB(K))*(QDB(K+1)-QDB(K))
#       /(QTDB(K+1)-QTDB(K)) -Q(N) -F(N)) / E(N)
    RETURN
15 CONTINUE
    DELY=(QDB(NQDB)-Q(N)-F(N))/E(N)
    RETURN

```

```

C
C   INTERPOLATE THE STAGE HYDROGRAPH
C
20 IF(TIME .GE. YTDB(1)) GO TO 22
   DELY=YDB(1)-Y(N)
   RETURN
22 DO 25 K=1,NYDB1
   IF(.NOT.(TIME .GE. YTDB(K) .AND.
#      TIME .LT. YTDB(K+1))) GO TO 25
   DELY=YDB(K)+(TIME-YTDB(K))*(YDB(K+1)-YDB(K))
#      /(YTDB(K+1)-YTDB(K)) -Y(N)
   RETURN
25 CONTINUE
   DELY=YDB(NYDB)-Y(N)
   RETURN

C
C   FLOW IS LOCALLY UNIFORM : MANNING'S EQ
C
30 CKYS=CKS5*R(N)**0.6666667
   DELY=(-Q(N)+CKYS*A(N)-F(N))/(E(N)-(1.666667*B(N)
#      -0.666667*R(N)*DPY)*CKYS)
   RETURN
   END

SUBROUTINE UPBC
COMMON /C02/ Q(34),V(34),Y(34)
COMMON /C03/ E(34),F(34),ITYP(34)
COMMON /C05/ QTUB(10,2),QUB(10,2),NQUB(2),NCHAN
COMMON /C06/ N,NT,TIME,I,KT,MNT1,LE

DATA NCH/1/

C
C   INTERPOLATE THE DISCHARGE HYDROGRAPH
C
1 NQUB1=NQUB(NCH)-1
  E(1)=0.0
  IF(TIME .GE. QTUB(1,NCH)) GO TO 5
  F(1)=QUB(1,NCH)-Q(1)
  GO TO 20
5 DO 10 K=1,NQUB1
  IF(.NOT.(TIME .GE. QTUB(K,NCH) .AND.
#      TIME .LT. QTUB(K+1,NCH))) GO TO 10
  F(1)=QUB(K,NCH)+(TIME-QTUB(K,NCH))*(QUB(K+1,NCH)-QUB(K,NCH))
#      /(QTUB(K+1,NCH)-QTUB(K,NCH)) -Q(1)
  GO TO 20
10 CONTINUE
  F(1)=QUB(NQUB(NCH),NCH)-Q(1)
20 NCH=NCH+1
  IF(NCH .GT. NCHAN) NCH=1
  RETURN
  END

SUBROUTINE POND
COMMON /C02/ Q(34),V(34),Y(34)
COMMON /C06/ N,NT,TIME,I,KT,MNT1,LE
COMMON /C09/ GRAV,SWI,DELTAT,ALPHA,BETA,THETA
COMMON /C12/ AA,BB,CC,DD,GG,AA1,BB1,CC1,DD1,GG1
COMMON /C14/ SURF,YBASE
AA1=0.0
BB1=-THETA
IF(Y(1) .LE. YBASE) GO TO 5
CC1=SURF/DELTAT
GO TO 10

```



```

5 CC1=0.0
10 DD1=-THETA
   GG1=Q(I+1)-Q(I)
   AA=1.0
   BB=0.0
   CC=1.0
   DD=0.0
   GG=Y(I)-Y(I+1)
   RETURN
   END

```

```

SUBROUTINE WEIR
COMMON /C02/ Q(34),V(34),Y(34)
COMMON /C06/ N,NT,TIME,I,KT,MNT1,LE
COMMON /C09/ GRAV,SW1,DELTAT,ALPHA,BETA,THETA
COMMON /C11/ WY,WB,CMU
COMMON /C12/ AA,BB,CC,DD,GG,AA1,BB1,CC1,DD1,GG1
IF(NT .GT. 1) GO TO 5
CMBG=CMU*WB*(2.0*GRAV)**0.5
CMBG3=CMBG*0.57735
CMBGE=CMBG*10.0
5 AA1=0.0
  BB1=1.0
  CC1=0.0
  DD1=1.0
  GG1=Q(I)-Q(I+1)
  BB=0.0
  DD=1.0
  IF(Q(I) .LT. 0.0) GO TO 10
C
C   POSITIVE Q
C
  YUS=Y(I)
  YDS=Y(I+1)
  GO TO 20
C
C   NEGATIVE Q
C
10 YUS=Y(I+1)
  YDS=Y(I)
20 YUSW=YUS-WY
  YDSW=YDS-WY
  YUSDS=YUS-YDS
  IF(YDSW .GT. 0.6666667*YUSW) GO TO 30
C
C   FREE FLOW
C
  DQUS=CMBG3*YUSW**0.5
  DQDS=0.0
  QW=0.6666667*DQUS*YUSW
  GO TO 50
C
C   FLOODED WEIR
C
30 IF(ABS(YUSDS) .LT. 0.01) GO TO 40
  YUSDS5=YUSDS**0.5
  T=0.5*YDSW/YUSDS5
  DQUS=CMBG*T
  DQDS=CMBG*(YUSDS5-T)
  QW=CMBG*YUSDS5*YDSW
  GO TO 50
40 DQUS=CMBGE*YDSW
  DQDS=CMBGE*(YUSDS-YDSW)
  QW=DQUS*YUSDS
50 IF(Q(I) .LT. 0.0) GO TO 60

```

```

AA=DQDS
CC=-DQUS
GG=Q(I)-QW
RETURN
60 AA=-DQUS
CC=DQDS
GG=Q(I)+QW
RETURN
END

```

```

SUBROUTINE JUNC
COMMON /C02/ Q(34),V(34),Y(34)
COMMON /C03/ E(34),F(34),ITYP(34)
COMMON /C06/ N,NT,TIME,I,KT,MNT1,LE
COMMON /C10/ NNOD,NOD(2),NOD1(2)
DATA EJUNC,FJUNC/2*0.0/
5 DO 10 K=1,NNOD
  IF(I .EQ. NOD(K)) GO TO 15
10 CONTINUE
15 EJUNC=EJUNC+E(I)
  FJUNC=FJUNC+Q(I)+E(I)*(Y(NOD1(K))-Y(I))+F(I)
  IF(K .NE. NNOD) RETURN
  E(NOD1(K))=EJUNC
  F(NOD1(K))=FJUNC-Q(NOD1(K))
  EJUNC=0.0
  FJUNC=0.0
  RETURN
END

```

```

SUBROUTINE ICE
COMMON /C06/ N,NT,TIME,I,KT,MNT1,LE
COMMON /C15/ ICEFLG(34),T(34),C(34),TH(34)
IF(NT .GT. 1) GO TO 20
DO 10 I=1,N
  ICEFLG(I)=0
  IF(TH(I) .GT. 0.0) ICEFLG(I)=1
10 CONTINUE
20 IF(KT .LT. 1) RETURN
DO 30 I=1,N
  IF(TH(I) .GT. 0.0) ICEFLG(I)=1
30 CONTINUE
RETURN
END

```

```

SUBROUTINE TEMP

C
C VERTICALLY AVERAGED WATER TEMPERATURE AND ICE CONCENTRATION
C ARE COMPUTED USING THE CHARACTERISTIC BASED H-P 4TH ORDER
C INTERPOLATION SCHEME.
C

COMMON /C01/ A(34),B(34),BW(34),H(34),R(34),S(34),
# CK(34),DKY(34),CKST(34),Z(34)
COMMON /C02/ Q(34),V(34),Y(34)
COMMON /C06/ N,NT,TIME,I,KT,MNT1,LE
COMMON /C09/ GRAV,SWI,DELTAT,ALPHA,BETA,THETA
COMMON /C13/ DELX(34),X(34)
COMMON /C15/ ICEFLG(34),T(34),C(34),TH(34)
COMMON /C16/ TA(200),TTUB(200),TO(34),CTUB(200),CO(34)
COMMON /C17/ ROU,HWA,CLATNT
DIMENSION BO(34),HXO(34),HX(34),VO(34),VXO(34),VX(34)
DIMENSION ALPO(34),ALP(34),TXO(34),TX(34),TT(200)
DIMENSION CXO(34),CX(34),CT(200)
IF(KT .GT. 1) GO TO 120

```

```

C
C   READ AND DEFINE THE INITIAL VALUES.
C
  READ(1,*) HWA,ROU,SPHT,CLATNT
  WRITE(6,500) HWA,ROU,SPHT,CLATNT
  HWA=HWA*10000./ (24.*3600.)
  ROU=ROU*1.E6
  CALL AIRTMP
  CALL TICOND
  CALL TUPBC
  CALL CICOND
  CALL CUPBC
  CALL DIFFX(TO, TXO, N)
  CALL DIFFT(TTUB, TT, MNT1)
  N1=N-1
  DO 100 I=1, N1
    IF(ICEFLG(I) .NE. 0) GO TO 105
100  CONTINUE
105  LE=I
    CALL DIFFX(CO, CXO, N)
    CALL DIFFT(CTUB, CT, MNT1)
    CST=HWA/(ROU*SPHT)
    EPS=HWA/(ROU*CLATNT)
    DTAT2=DELTAT*0.5
    EPST2=EPS*DTAT2
110  DO 111 I=1, N
    HO(I)=H(I)
    VO(I)=V(I)
    T(I)=TO(I)
    TX(I)=TXO(I)
    C(I)=CO(I)
    CX(I)=CXO(I)
111  ALPO(I)=CST/HO(I)
    CALL DIFFX(HO, HXO, N)
    CALL DIFFX(VO, VXO, N)
    RETURN
120  CALL DIFFX(H, HX, N)
    CALL DIFFX(V, VX, N)
    KT1=KT-1
    DO 122 I=1, N
122  ALP(I)=CST/H(I)
    T(I)=TTUB(KT)
    TX(I)=(ALP(I)*(TA(KT)-T(I))-TT(KT))/V(I)
C    TX(I)=TT(KT)/V(I)
    C(I)=CTUB(KT)
    CX(I)=(EPS*TA(KT)/H(I)+CT(KT))/V(I)
    NOICE=LE
    IF(ICEFLG(LE) .NE. 1) NOICE=LE+1
    DO 200 I=2, NOICE
C
C   COMPUTE THE TRAJECTORY OF THE CHARACTERISTIC LINE USING THE
C   TIME AVERAGED WATER VELOCITIES.
C
    XSI=X(I)-DTAT2*(V(I)+VO(I-1))
    IF(XSI .LT. 0.0) GO TO 150
    ITR=1
125  DO 130 L=2, I
    IF(XSI .GE. X(L-1) .AND. XSI .LE. X(L)) GO TO 135
130  CONTINUE
    WRITE(6,300)
300  FORMAT(///,1X,20(' '), 'XSI IS OUT OF BOUNDARY')
    STOP 200
135  L1=L-1
    QCON=DTAT2*(VO(L)-VO(L1))/DELX(L1)
    XSI=(X(I)-DTAT2*(V(I)+VO(L))+QCON*X(L))/(QCON+1.0)
    IF(XSI .LT. 0.0) GO TO 150
    IF(XSI .GE. X(L1) .AND. XSI .LE. X(L) .OR. ITR .GE. 3) GO TO 140
    ITR=ITR+1
    GO TO 125

```

```

C
C   TRAJECTORY OF THE CHARACTERISTIC LINE FALLS WITHIN THE CHANNEL
C   REACH.
C   INTERPOLATION ON SPACE IS NEEDED.
C
140 TAU=(X(L)-XSI)/DELX(L1)
    TAU2=TAU*TAU
C
C   COMPUTE THE COEFFICIENTS OF THE 4TH ORDER H-P INTERPOLATION
C   SCHEME BASED ON THE HERMITE QUBIC POLYNOMIAL.
C
    A1=TAU2*(3.-2.*TAU)
    A2=1.-A1
    A3=TAU2*(1.-TAU)*DELX(L1)
    A4=-TAU*(1.-TAU)**2*DELX(L1)
    B1=6.0*TAU*(TAU-1.)/DELX(L1)
    B2=-B1
    B3=TAU*(3.*TAU-2.)
    B4=(TAU-1.)*(3.*TAU-1.)
    IF(TO(I) .LE. 0.0) GO TO 145
C
C   LINEAR INTERPOLATION FOR THE FOLLOWING QUANTITIES.
C
143 ALPXSI=(1.-TAU)*ALPO(L)+TAU*ALPO(L1)
    VXSI=(1.-TAU)*VO(L)+TAU*VO(L1)
    VXXSI=(1.-TAU)*VXO(L)+TAU*VXO(L1)
    HXSI=(1.-TAU)*HO(L)+TAU*HO(L1)
    HXXSI=(1.-TAU)*HXO(L)+TAU*HXO(L1)
C
C   COMPUTE THE WATER TEMPERATURE AND ITS SPACE DERIVATIVE.
C
    TXSI=A1*TO(L1)+A2*TO(L)+A3*TXO(L1)+A4*TXO(L)
    T(I)=((1.-DTAT2*ALPXSI)*TXSI+DTAT2*(ALP(I)*TA(KT)+ALPXSI*TA(KT1)))
    # / (1.+DTAT2*ALP(I))
    TXXSI=B1*TO(L1)+B2*TO(L)+B3*TXO(L1)+B4*TXO(L)
    TX(I)=((1.-DTAT2*(VXXSI+ALPXSI))*TXXSI+DTAT2*((TA(KT1)-TXSI)
    # *ALPXSI+HXXSI/HXSI+(TA(KT)-T(I))*ALP(I)*HX(I)/H(I)))
    # / (1.+DTAT2*(VX(I)+ALP(I)))
    GO TO 200
145 IF(CO(I) .LE. 0.0 .AND. TA(KT) .GT. 0.0) GO TO 143
C
C   LINEAR INTERPOLATION FOR THE FOLLOWING QUANTITIES.
C
    VXXSI=(1.-TAU)*VXO(L)+TAU*VXO(L1)
    HXSI=(1.-TAU)*HO(L)+TAU*HO(L1)
    HXXSI=(1.-TAU)*HXO(L)+TAU*HXO(L1)
C
C   COMPUTE THE ICE CONTERATION AND ITS SPACE DERIVATIVE.
C
    CXSI=A1*CO(L1)+A2*CO(L)+A3*CXO(L1)+A4*CXO(L)
    C(I)=CXSI-EPST2*(TA(KT)/H(I)+TA(KT1)/HXSI)
    CXXSI=B1*CO(L1)+B2*CO(L)+B3*CXO(L1)+B4*CXO(L)
    CX(I)=((1.-DTAT2*VXXSI)*CXXSI
    # +EPST2*(TA(KT)*HX(I)/H(I)**2+TA(KT1)*HXXSI/HXSI**2))
    # / (1.+DTAT2*VX(I))
    GO TO 200
150 CONTINUE
C
C   TRAJECTORY OF THE CHARACTERISTIC LINE FALLS ON THE U/S BOUNDARY.
C   INTERPOLATION ON TIME IS NEEDED.
C
    CQ=(VO(1)-V(1))/DELTAT
    CP=V(1)+V(I)
    CR=-2.*X(I)
    IF(CQ .NE. 0.0) GO TO 155
    ETAS=-CR/CP

```

```

      GO TO 156
155 ETAS=(-CP+(CP*UP-4.*CQ*CR)**0.5)/(2.*CQ)
156 XLAM=ETAS/DELTAT
      IF(XLAM .LE. 1.0) GO TO 160
      WRITE(6,400)
400  FORMAT(///,5X,20(' '), '  FAIL TO LOCATE THE STARTING POINT')
      STOP 300
160 ETAS2=ETAS*0.5
      IF( TO(I) .LE. 0.0) GO TO 165
C
C      LINEAR INTERPOLATION FOR THE FOLLOWING QUANTITIES.
C
162 TETA=(1.-XLAM)*T(1)+XLAM*TO(1)
   TAETA=(1.-XLAM)*TA(KT)+XLAM*TA(KT1)
   TTETA=(1.-XLAM)*TT(KT)+XLAM*TT(KT1)
   VETA=(1.-XLAM)*V(1)+XLAM*VO(1)
   VXETA=(1.-XLAM)*VX(1)+XLAM*VXO(1)
   HETA=(1.-XLAM)*H(1)+XLAM*HO(1)
   HXETA=(1.-XLAM)*HX(1)+XLAM*HXO(1)
   ALPETA=(1.-XLAM)*ALP(1)+XLAM*ALPO(1)
C
C      COMPUTE THE WATER TEMPERATURE AND ITS SPACE DERIVATIVE.
C
      T(I)=((1.-ETAS2*ALPETA)*TETA+ETAS2*(ALPETA*TAETA+ALP(I)*TA(KT)))
      # / (1.+ETAS2*ALP(I))
      TXETA=(ALPETA*(TAETA-TETA)-TTETA)/VETA
      TX(I)=((1.-ETAS2*(VXETA+ALPETA))*TXETA+ETAS2*((TAETA-TETA)
      # *ALPETA*HXETA/HETA+(TA(KT)-T(I))*ALP(I)*HX(I)/H(I)))
      # / (1.+ETAS2*(VX(I)+ALP(I)))
      GO TO 200
165 IF(CO(I) .LE. 0.0 .AND. TA(KT) .GT. 0.0) GO TO 162
C
C      LINEAR INTERPOLATION FOR THE FOLLOWING QUANTITIES.
C
      CETA=(1.-XLAM)*C(1)+XLAM*CO(1)
      CTETA=(1.-XLAM)*CT(KT)+XLAM*CT(KT1)
      TAETA=(1.-XLAM)*TA(KT)+XLAM*TA(KT1)
      VETA=(1.-XLAM)*V(1)+XLAM*VO(1)
      VXETA=(1.-XLAM)*VX(1)+XLAM*VXO(1)
      HETA=(1.-XLAM)*H(1)+XLAM*HO(1)
      HXETA=(1.-XLAM)*HX(1)+XLAM*HXO(1)
C
C      COMPUTE THE ICE CONCENTRATION AND ITS SPACE DERIVATIVE.
C
      C(I)=CETA-EPS*ETAS2*(TA(KT)/H(I)+TAETA/HETA)
      CXETA=-(EPS*TAETA/HETA+CTETA)/VETA
      CX(I)=(1.-ETAS2*VXETA)*CXETA
      # +EPS*ETAS2*(TA(KT)*HX(I)/H(I)**2+TAETA*HXETA/HETA**2)
200 CONTINUE
      DO 210 I=1,N
      HO(I)=H(I)
      HXO(I)=HX(I)
      VO(I)=V(I)
      VXO(I)=VX(I)
      TO(I)=T(I)
      TXO(I)=TX(I)
      CO(I)=C(I)
      CXO(I)=CX(I)
      ALPO(I)=ALP(I)
210 CONTINUE
      RETURN
500 FORMAT(
      # ' < THERMAL CONDITION > ',//
      # ' Energy exchange coeff. at the air-water interface = ',
      #       F6.2, ' cal/cm**2.day.C',/
      # ' Density of water = ',F5.2, ' g/cm**3',/
      # ' Specific heat of water = ',F5.2, ' cal/g.C',/
      # ' Latent heat of fusion of ice = ',F6.2, ' cal/g',//)
      END

```

```

SUBROUTINE DIFFX(F,FX,N)
C
C COMPUTE THE SPACE DERIVATIVE USING THE WEIGHTED DIFFERENCE.
C
COMMON /C13/ DELX(34),X(34)
DIMENSION F(1),FX(1)
N1=N-1
FX(1)=(F(2)-F(1))/DELX(1)
FX(N)=(F(N)-F(N1))/DELX(N1)
DO 10 I=2,N1
I1=I-1
S1=(F(I)-F(I1))/DELX(I1)
S2=(F(I+1)-F(I))/DELX(I)
10 FX(I)=(S1*DELX(I)+S2*DELX(I1))/(DELX(I1)+DELX(I))
RETURN
END

SUBROUTINE DIFFT(F,FT,NT)
C
C COMPUTE THE TIME DERIVATIVE USING THE CENTRAL DIFFERENCE.
C
COMMON /C09/ GRAV,SWI,DELTAT,ALPHA,BETA,THETA
DIMENSION F(1),FT(1)
NT1=NT-1
FT(1)=(F(2)-F(1))/DELTAT
FT(NT)=(F(NT)-F(NT1))/DELTAT
DO 10 J=2,NT1
10 FT(J)=(F(J+1)-F(J-1))/(2.*DELTAT)
RETURN
END

SUBROUTINE AIRTMP
C
C DEFINE THE BOUNDARY CONDITION FOR THE AIR TEMPERATURE.
C
COMMON /C06/ N,NT,TIME,I,KT,MNT1,LE
COMMON /C09/ GRAV,SWI,DELTAT,ALPHA,BETA,THETA
COMMON /C16/ TA(200),TTUB(200),TO(34),CTUB(200),CO(34)
READ(1,*) CONTA
DO 10 J=1,MNT1
10 TA(J)=CONTA
RETURN
END

SUBROUTINE TICOND
C
C DEFINE THE INITIAL CONDITION FOR THE WATER TEMPERATURE.
C
COMMON /C06/ N,NT,TIME,I,KT,MNT1,LE
COMMON /C16/ TA(200),TTUB(200),TO(34),CTUB(200),CO(34)
READ(1,*) CONTO
DO 10 I=1,N
10 TO(I)=CONTO
RETURN
END

```

```

SUBROUTINE TUPBC
C
C   DEFINE THE U/S B.C. FOR THE WATER TEMPERATURE.
C
COMMON /C06/ N,NT,TIME,I,KT,MNT1,LE
COMMON /C09/ GRAV,SWI,DELTAT,ALPHA,BETA,THETA
COMMON /C16/ TA(200),TTUB(200),TO(34),CTUB(200),CO(34)
READ(1,*) CONTUB
DO 10 J=1,MNT1
C 10 TTUB(J)=5.-5.*SIN(2.*3.141592*(J-1)*DELTAT/36000.)
10 TTUB(J)=CONTUB
RETURN
END

SUBROUTINE CICOND
C
C   DEFINE THE INITIAL CONDITION FOR THE ICE CONCENTRATION.
C
COMMON /C06/ N,NT,TIME,I,KT,MNT1,LE
COMMON /C16/ TA(200),TTUB(200),TO(34),CTUB(200),CO(34)
DO 10 I=1,N
10 CO(I)=0.0
RETURN
END

SUBROUTINE CUPBC
C
C   DEFINE THE U/S B.C. FOR THE ICE CONCENTRATION.
C
COMMON /C06/ N,NT,TIME,I,KT,MNT1,LE
COMMON /C09/ GRAV,SWI,DELTAT,ALPHA,BETA,THETA
COMMON /C16/ TA(200),TTUB(200),TO(34),CTUB(200),CO(34)
DO 10 J=1,MNT1
10 CTUB(J)=0.0
RETURN
END

SUBROUTINE ICECVR
C
C   SIMULATION OF THE ICE COVER FORMATION
C
COMMON /C01/ A(34),B(34),BW(34),H(34),R(34),S(34),
# CK(34),DKY(34),CKST(34),Z(34)
COMMON /C02/ Q(34),V(34),Y(34)
COMMON /C06/ N,NT,TIME,I,KT,MNT1,LE
COMMON /C09/ GRAV,SWI,DELTAT,ALPHA,BETA,THETA
COMMON /C13/ DELX(34),X(34)
COMMON /C15/ ICEFLG(34),T(34),C(34),TH(34)
IF(KT .GT. 1) GO TO 5
N1=N-1
READ(1,*) FRMAX,FRMIN,THFLOE,ALPS,EI,EP,SWI
EC=EP+(1.-EP)*EI
WRITE(6,100) FRMAX,FRMIN,THFLOE,ALPS,EI,EP,EC,SWI
CONA=(2.*(1.-EC)*(1.-SWI))**0.5
5 CVOL=ALPS*C(LE)*Q(LE)*DELTAT
IF(CVOL .LE. 0.0) RETURN
FR=V(LE)/(GRAV*H(LE))**0.5
IF(FR .GT. FRMAX) GO TO 60
IF(FR .GT. FRMIN) GO TO 10
C
C   FROUDE NO. IS LESS THAN MINIMUM FROUDE NO.

```

```

C   THE THICKNESS OF THE ICE COVER WILL BE EQUAL TO THE THICKNESS
C   OF ICE FLOE.
C
C   THMAX=THFLOE
C   GO TO 35
C
C   FROUDE NO. IS BETWEEN THE MAXIMUM AND THE MINIMUM.
C   COMPUTE THE ICE COVER THICKNESS BASED ON THE ICE JAM THEORY.
C
10  ITER=1
    W=0.0
20  F=W*(W*W-1.0)+FR/CONA
    FD=3.0*W*W-1.0
    W=W-F/FD
    IF(ABS(F) .LT. 1.E-6 .OR. ITER .GE. 10) GO TO 30
    ITER=ITER+1
    GO TO 20
30  THMAX=W*W*H(LE)
35  DTH=CVOL/(DELX(LE)*(B(LE)+B(LE+1))*0.5)
    IF(TH(LE)+DTH .LT. THMAX) GO TO 50
    DVOL=CVOL-CVOL*(THMAX-TH(LE))/DTH
    TH(LE)=THMAX
    C(LE+1)=0.0
    IF(LE .EQ. N1) TH(N)=TH(LE)
    LE=LE+1
    IF(LE .GT. 0) GO TO 40
    WRITE(6,36)
36  FORMAT(////, ' ***** ICE COVER REACHES THE U/S *****', /
#      ' ***** PROGRAM TERMINATED *****', /)
    STOP
40  TH(LE)=DVOL/(DELX(LE)*(B(LE)+B(LE+1))*0.5)
    RETURN
50  TH(LE)=TH(LE)+DTH
    C(LE+1)=0.0
    IF(LE .EQ. N1) TH(N)=TH(LE)
    RETURN
60  IF(LE .NE. N1) GO TO 65
    WRITE(6,63) FR
63  FORMAT(////, ' ***** FR NO. OF D/S = ', F5.2,
#      ' IS GREATER THAN THE FRMAX : NO ICE COVER CAN BE FORMED
#      *****', /)
    STOP
C
C   FROUDE NO. IS GREATER THAN MAXIMUM FROUDE NO.
C   FIND THE NEAREST D/S SECTION WHERE THE FROUDE NO. IS LESS THAN
C   MAXIMUM FROUDE NO. AND THEN ACCUMULATE THE BRAZIL ICE AT THAT
C   SECTION.
C
65  LE1=LE+1
    DO 70 K=LE1,N1
        FR=V(K)/((GRAV*H(K))**0.5)
        IF(FR .LE. FRMAX) GO TO 80
70  CONTINUE
80  DTH=CVOL/(DELX(K)*(B(K)+B(K+1))*0.5)
    TH(K)=TH(K)+DTH
    IF(K .EQ. N1) TH(N)=TH(K)
    RETURN
100 FORMAT(
#  ' < ICE CONDITION >', /
#  ' Maximum Fr No. at which the ice cover can not progress = ',
#      F5.2, /
#  ' Minimum Fr No. for the formation of ice cover = ', F5.2, /
#  ' The thickness of ice floe = ', F5.3, ' m', /
#  ' The ratio of the surface ice discharge to the total ice',
#  ' discharge = ', F4.2, /
#  ' Porosity of individual ice floes = ', F5.3, /
#  ' Porosity of the ice accumulation between ice floes = ', F5.3, /

```



```
# Porosity of the ice accumulation = ',F5.3,/
# Specific gravity of the ice = ',F5.3,/)
END
```

```
SUBROUTINE THICON
COMMON /C06/ N,NT,TIME,I,KT,MNT1,LE
COMMON /C15/ ICEFLG(34),T(34),C(34),TH(34)
DO 10 I=1,N
10 TH(I)=0.0
RETURN
END
```

```
SUBROUTINE CONDOC
COMMON /C06/ N,NT,TIME,I,KT,MNT1,LE
COMMON /C09/ GRAV,SWI,DELTAT,ALPHA,BETA,THETA
COMMON /C15/ ICEFLG(34),T(34),C(34),TH(34)
COMMON /C16/ TA(200),TTUB(200),TO(34),CTUB(200),CO(34)
COMMON /C17/ ROU,HWA,CLATNT
IF(KT.GT. 1) GO TO 10
READ(1,*) HIA,TCI
WRITE(6,200) HIA,TCI
ROU=ROU*SWI
HIA=HIA*10000./((24.*3600.))
TCI=TCI*100.
DTRC=DELTAT/(ROU*CLATNT)
10 DO 100 I=LE,N
IF(TH(I).LE. 0.0) GO TO 100
TS=TA(KT)*HIA*TH(I)/(HIA*TH(I)+TCI)
IF(TS.GT. 0.0) GO TO 50
C DTH=-(TS*TCI/TH(I)+HWI*T(I))*DTRC
DTH=-TS*TCI/TH(I)*DTRC
TH(I)=TH(I)+DTH
GO TO 100
C DTH=-(HIA*TA(KT)+HWI*T(I))*DTRC
50 DTH=-HIA*TA(KT)*DTRC
TH(I)=TH(I)+DTH
IF(TH(I).LT. 0.0) TH(I)=0.0
100 CONTINUE
RETURN
200 FORMAT(
# Energy exchange coeff. at the air-ice interface = ',
# F6.2,' cal/cm**2.day.C',/
# Thermal conductivity of ice = ',F7.4,' cal/cm.sec.C',/)
END
```

REPORT DOCUMENTATION PAGE

Form Approved
OMB No. 0704-0188

Public reporting burden for this collection of information is estimated to average 1 hour per response, including the time for reviewing instructions, searching existing data sources, gathering and maintaining the data needed, and completing and reviewing the collection of information. Send comments regarding this burden estimate or any other aspect of this collection of information, including suggestion for reducing this burden, to Washington Headquarters Services, Directorate for Information Operations and Reports, 1215 Jefferson Davis Highway, Suite 1204, Arlington, VA 22202-4302, and to the Office of Management and Budget, Paperwork Reduction Project (0704-0188), Washington, DC 20503.

1. AGENCY USE ONLY (Leave blank)		2. REPORT DATE May 1993		3. REPORT TYPE AND DATES COVERED	
4. TITLE AND SUBTITLE Flow Regulation for Controlled River-Ice Formation				5. FUNDING NUMBERS	
6. AUTHORS Subash C. Jain, Robert Ettema and Inbo Park					
7. PERFORMING ORGANIZATION NAME(S) AND ADDRESS(ES) Iowa Institute of Hydraulic Research University of Iowa Iowa City, Iowa				8. PERFORMING ORGANIZATION REPORT NUMBER CRREL Report 93-3	
9. SPONSORING/MONITORING AGENCY NAME(S) AND ADDRESS(ES) U.S. Army Cold Regions Research and Engineering Laboratory 72 Lyme Road Hanover, New Hampshire 03755-1290				10. SPONSORING/MONITORING AGENCY REPORT NUMBER	
11. SUPPLEMENTARY NOTES					
12a. DISTRIBUTION/AVAILABILITY STATEMENT Approved for public release; distribution is unlimited. Available from NTIS, Springfield, Virginia 22161.				12b. DISTRIBUTION CODE	
13. ABSTRACT (Maximum 200 words) Results are presented of a study to determine appropriate methods of flow modification for mitigating ice jam formation in navigable rivers. Based on a review of alternative methods for flow modification, it is concluded that for many rivers, especially large ones, the most appropriate method involves controlled ice-cover formation through the regulation of river flow. Flow discharge and stages would be regulated by controlling the flow releases from reservoirs and flow stages at river dams, such that optimal flow conditions prevail for rapid formation, and subsequent maintenance, of an accumulation ice cover over river reaches in which potentially large amounts of frazil ice may grow. Accumulation covers would be formed of frazil ice pans and floes and, if appropriate, broken ice conveyed from upstream. Existing dams, augmented where needed by navigable ice booms, could serve as retention structures for the development of accumulation covers. A preliminary indication of the feasibility of this method for controlling ice-cover formation on stage-regulated pools of the Ohio River is assessed through the use of a numerical model that simulates ice-cover formation from frazil ice. It is found that this approach holds promise for mitigating jam occurrence, although its implementation necessarily entails management of flow through major portions of the Ohio River. The results of the study are, to a limited extent, generalized to other rivers.					
14. SUBJECT TERMS Frazil ice Simulation models Waterways Ice cover Water-surface profiles River regulation Water temperature				15. NUMBER OF PAGES 58	
				16. PRICE CODE	
17. SECURITY CLASSIFICATION OF REPORT UNCLASSIFIED	18. SECURITY CLASSIFICATION OF THIS PAGE UNCLASSIFIED	19. SECURITY CLASSIFICATION OF ABSTRACT UNCLASSIFIED	20. LIMITATION OF ABSTRACT		